


Opinion formation and distribution in a bounded-confidence model on various networksX. Flora Meng,^{1,2} Robert A. Van Gorder,¹ and Mason A. Porter^{1,3,4,*}¹*Mathematical Institute, University of Oxford, Oxford OX2 6GG, United Kingdom*²*Department of Electrical Engineering and Computer Science, Massachusetts Institute of Technology, Cambridge, Massachusetts 02139, USA*³*CABDyN Complexity Centre, University of Oxford, Oxford OX1 1HP, United Kingdom*⁴*Department of Mathematics, University of California, Los Angeles, California 90095, USA* (Received 9 January 2017; revised manuscript received 23 December 2017; published 22 February 2018)

In the social, behavioral, and economic sciences, it is important to predict which individual opinions eventually dominate in a large population, whether there will be a consensus, and how long it takes for a consensus to form. Such ideas have been studied heavily both in physics and in other disciplines, and the answers depend strongly both on how one models opinions and on the network structure on which opinions evolve. One model that was created to study consensus formation quantitatively is the Deffuant model, in which the opinion distribution of a population evolves via sequential random pairwise encounters. To consider heterogeneity of interactions in a population along with social influence, we study the Deffuant model on various network structures (deterministic synthetic networks, random synthetic networks, and social networks constructed from Facebook data). We numerically simulate the Deffuant model and conduct regression analyses to investigate the dependence of the time to reach steady states on various model parameters, including a confidence bound for opinion updates, the number of participating entities, and their willingness to compromise. We find that network structure and parameter values both have important effects on the convergence time and the number of steady-state opinion groups. For some network architectures, we observe that the relationship between the convergence time and model parameters undergoes a transition at a critical value of the confidence bound. For some networks, the steady-state opinion distribution also changes from consensus to multiple opinion groups at this critical value.

DOI: [10.1103/PhysRevE.97.022312](https://doi.org/10.1103/PhysRevE.97.022312)**I. INTRODUCTION**

Social interactions play a central role in the process of decision making and opinion formation in populations of humans and other animals [1,2]. Discussions among acquaintances, coworkers, friends, and family members often lead interlocutors to adjust their viewpoints on politics, participation in a social movement, adoption of technological innovations, or other things [3–7]. Indeed, trying to forecast collective opinion formation in a population from attributes of individuals is one of the most important problems in the social sciences [8,9]. Consensus dynamics is also a key problem in areas such as control theory [10,11] and collective dynamics more generally [12]. From a physical and mathematical standpoint, the study of opinion dynamics is one of the key motivating examples for examining the effects of network structure on dynamical processes on networks [13].

There are various methods for studying opinion formation in social networks, such as through Bayesian learning or generative social-interaction mechanisms [14]. Bayesian updating requires some unrealistic assumptions about individuals' knowledge and reasoning ability, and it becomes computationally infeasible in complex settings [1,14]. Even in opinion models that do not suffer from these issues, there remains significant arbitrariness in the choice of specific models and parameters to use, and different choices can lead

to markedly (and qualitatively) different results [14,15]. A substantial amount of work on non-Bayesian approaches to opinion formation employs models and tools from dynamical systems, probability theory, and statistical physics [8]. Moreover, a major theme in statistical physics is how global properties can emerge from local rules, which is similar to the question in the social sciences of how the collective opinion of a population evolves as a result of individual attitudes and the mutual influence of individuals on each other [16]. Some notable generative models of opinion formation include voter models [17–20], majority-rule models [21], models based on social-impact theory [22,23], the Sznajd model [24,25], and bounded-confidence models [26–29].

Bounded-confidence models, first introduced (to our knowledge) by Deffuant *et al.* [26,30] and Hegselmann and Krause [27,28], capture the notion of a tolerance threshold based on experimental social psychology [31,32]. Bounded confidence reflects the psychological concept of *selective exposure*, which refers to an individual's tendency to favor information that supports his/her views while neglecting conflicting arguments [33,34]. The Deffuant model and the Hegselmann–Krause (HK) model both consider a set of agents who hold continuous opinions that can change. Agents are connected to each other by an interaction network, and neighboring agents adjust their opinions at discrete time steps whenever their opinions are sufficiently close to each other. The two models differ primarily in how they model communication. In the HK model, agents interact with all of their compatible neighbors simultaneously at each time step, and they update their opinions to agree with

*mason@math.ucla.edu

the mean opinion of these neighbors. In contrast, the Deffuant model adopts a sequential updating rule and can be viewed as a discrete-time repeated game that is played in pairwise fashion among a set of agents until the agents' opinions converge to either a single opinion or multiple opinions [1,35,36]. One can also tune the speed at which opinions converge in the Deffuant model using an additional parameter, sometimes called a *cautiousness parameter*, that describes openness to compromise. The Deffuant model was developed to study opinion-formation processes in large populations in which individual agents interact in pairs, whereas the HK model is suitable for contexts such as meetings with many participants. Despite the differences in interaction mechanisms in the two models, the original versions of the Deffuant and HK models have identical sets of stable opinion configurations [37]. The fact that there are many such configurations makes this result especially interesting. Two questions have drawn considerable attention: (1) How does the parameter space influence the number of steady-state opinion groups, where no further changes in opinions are possible? (2) How long does it take for a system to reach steady state [26,30,38–40]?

The study of opinion-formation processes has traditionally considered an opinion to be a discrete variable, which is a reasonable assumption for some applications. For instance, the classical voter model [17,18] has a binary variable that specifies one's decision in a vote. However, it is important to develop models that incorporate more nuanced opinions, and the Deffuant and HK models both have a continuous opinion space, as an individual's stance on a specific matter can vary smoothly from one extreme to another in many real-world scenarios [8]. For instance, a political position (on a single dimension) is not typically simply "left" or "right" but somewhere in between two extremes.

Although the Deffuant model may seem simple, analytical results about its convergence rate and steady-state behavior are hard to obtain in general, and most conclusions rely on Monte Carlo simulations. It has been shown numerically, for a few values of the cautiousness parameter, that consensus occurs for large confidence-bound values on complete graphs with a probability close to 1 in the large-population limit, whereas multiple opinion groups persist at steady state for low confidence bounds [30,38,40,41]. Different confidence-bound thresholds have been proposed for transitions from consensus to multiple opinion groups at steady state. When there are multiple groups, one can approximate the number of them by a function of the confidence-bound value [30,40]. Some numerical simulations have suggested that the time to reach steady-state opinions is proportional to the number of agents in a network [38]. Moreover, a larger value of the cautiousness parameter increases not only the convergence speed but also the number of agents who hold extreme opinions at steady state [38].

Some prior work has compared results for the Deffuant model on complete graphs with those on other networks. Results for complete graphs and square lattices are similar for large confidence-bound values, except that a few extreme opinions remain on square lattices at steady state [30]. The Deffuant model has also been simulated on random graphs [42] generated by Barabási–Albert (BA), Erdős–Rényi (ER), and Watts–Strogatz (WS) mechanisms [41,43–45]. However,

different assumptions and update rules are often used, and this poses a major barrier for comparing results across different networks.

There have also been efforts to study the Deffuant model from an analytical perspective using a density function for the agents in opinion space [39,46]. Assuming continuous time, such an approach adopts a classical strategy in statistical physics by deriving a rate equation (also called a "master equation") and can be interpreted as taking an infinite limit of the number of agents [47]. These derivations have not led to analytical solutions of the Deffuant model, but they require numerical integration of only a master equation, which is faster than running Monte Carlo simulations of the original model. One major finding of [46] is that the number of steady-state opinion groups grows via a series of bifurcations as the relative size of the confidence bound decreases. Moreover, major and minor opinion groups seem to emerge alternately. A bifurcating and alternating pattern was also observed in [47] through interactive discrete-time Markov chains. Unfortunately, however, analyses using a density-based method have relied on restrictive assumptions, such as homogeneous mixing and averaging agents' opinions as the model of compromise.

The Deffuant model itself also has limitations, and numerous efforts have been made to extend it to better reflect reality. For instance, the confidence bound imposes a boundary on interacting agents' decisions of whether or not to adjust their opinions. A small change in the difference between their opinions may lead to an entirely different decision. Therefore, some scholars have proposed the use of smooth confidence bounds, with which the attraction of agents decreases as their opinion difference increases [48,49]. Others have considered random deviations from the bounded-confidence assumption [50], spatial heterogeneities [51], heterogeneous tolerance thresholds [30,32,52], and time-dependent thresholds [30]. Additionally, the Deffuant model can be extended to incorporate vector-valued opinions, although this requires specifying how to compute a distance between opinions [53]. It is also worthwhile to study bounded-confidence models on networks (such as multilayer networks) with increasingly complicated structures [54], couple bounded-confidence models with the dynamics of social balance [55], and develop tractable models that incorporate various other social mechanisms and features (such as [56], which draws some motivation from fluid flow).

In this paper, we take a systematic approach to studying the Deffuant model on networks. Quantifying the confidence bound and the cautiousness of a population is an open question for many applications, and we hope to gain insight on these issues. Additionally, although various variants of the Deffuant model have been studied, prior work has usually considered specific parameter values and networks, and the conclusions in many studies have relied on visual inspection and various simplifying assumptions. We also make assumptions, of course, though we hope that our systematic approach will help inspire additional studies of the Deffuant model and its generalizations.

We explore the dependence of convergence time and the number of steady-state opinion groups on network structure, confidence bound, the number of participating agents, and their willingness to compromise. We conduct regression analyses to model convergence time as a function of the model parameters

and study the qualitative behavior of steady-state opinion groups. The results of such a regression analysis can be very helpful for suggesting subsequent studies to obtain a mechanistic understanding of results. The networks that we study fall into three categories. The first set of networks—complete graphs, cycles, prism graphs, square lattices, and complete multipartite graphs—are synthetic and deterministic. The Deffuant model has been much studied on complete graphs and square lattices due to their simple structures, and we extend this list of simple network structures and compare our simulation results on these networks with those on more complex architectures. From our simulations on deterministic graphs, we find that network topology and the parameter values of the Deffuant model appear to have an intertwined effect on convergence time, with the behavior of convergence time undergoing a transition at a confidence-bound threshold for some network structures. The second set of networks are random graphs (which are also synthetic), including cycles with random edges, prisms with random edges, and random graphs generated by an Erdős–Rényi model [57]. Due to their simplicity, these models are a good starting point for understanding the Deffuant model on random graphs. Our simulations suggest that the behavior of convergence time on random-graph models is similar to that on counterpart deterministic networks. The third set of networks are empirical and deterministic. In particular, we use two FACEBOOK100 networks, which are constructed using Facebook “friendship” data [58,59] and which are a type of network in which agents have discussions and their opinions can change over time. Using all three types of networks, we discuss the number of steady-state opinion groups and phenomena such as a confidence-bound threshold for a transition from consensus to multiple-opinion steady states. As in [26], we take into account all opinion groups when considering convergence time and the number of steady-state opinion groups. This corresponds to circumstances in which all opinions matter, as even small groups with antiestablishment opinions can be important [60]. See [38,47] for discussions about distinguishing major and minor opinion groups.

The rest of our paper is organized as follows. First, we introduce relevant definitions from network science, define the Deffuant model in mathematical terms, and present some important known results for the Deffuant model on networks. We then describe our methodology and introduce the networks and the approach that we use for numerical simulations. We then conduct regression analyses on our simulation results to explore the dependence of convergence time on network structure, confidence bound, the number of participating agents, and their cautiousness. We also discuss the phenomena that we observe about the number of steady-state opinion groups, and we comment on their sociological implications. In appendices, we give further details about our statistical analysis, present results for additional example graphs, and give the results of the best-fit parameters from the regressions.

II. BACKGROUND

In this section, we recall relevant definitions from network science. We then define the Deffuant model, give some intuition about its design, and present some important known results about the Deffuant model on networks.

A. Basic definitions from network science

A *network* is a set of items (called *nodes*) with connections (called *edges*) between them [42]. Many ideas in network science originated in graph theory, and we present some definitions [42,61] that are pertinent to our study. A *graph* G is a triple consisting of a *node set* $V(G)$, an *edge set* $E(G)$, and a relation that associates each edge with two nodes (not necessarily distinct), which are its *end points*. The simplest type of network is a graph. Two nodes are *adjacent*, and are called *neighbors* of each other, if and only if they are end points of the same edge. The *degree* of a node is equal to the number of its neighbors. A *regular graph* is a graph in which each node has the same degree. A *random-graph model* is a probability distribution on graphs that has some fixed parameters and generates networks randomly in other respects.

B. The Deffuant model

In the Deffuant model, randomly selected neighboring agents interact in a pairwise manner and make a compromise toward each other’s opinion whenever their opinion difference is below a given threshold. (Otherwise, their opinions do not change.) Consider a population of N agents, who are connected to each other socially via a network G ; and let $[a, b] \subset \mathbb{R}$ be the opinion space. At time $t \in \mathbb{N}$, suppose that each agent i holds a time-dependent opinion $x_i(t) \in [a, b]$. Given an initial opinion profile $\vec{x}(0) \in [a, b]^N$, a *confidence bound* $c \in [0, b - a]$, and a cautiousness parameter that we call the *multiplier* $m \in (0, 0.5]$, the *Deffuant model* is the random process $(\vec{x}(t))_{t \geq 0}$ defined as follows. At time t , a pair of neighboring agents, i and $j \neq i$, are selected uniformly at random (i.e., we select an edge uniformly at random) and update their opinions according to the equations

$$\begin{aligned} x_i(t+1) &= \begin{cases} x_i(t) + m\Delta_{j,i}(t), & \text{if } |\Delta_{i,j}(t)| < c, \\ x_i(t), & \text{otherwise,} \end{cases} \\ x_j(t+1) &= \begin{cases} x_j(t) + m\Delta_{i,j}(t), & \text{if } |\Delta_{i,j}(t)| < c, \\ x_j(t), & \text{otherwise,} \end{cases} \end{aligned} \quad (1)$$

where $\Delta_{j,i}(t) = x_j(t) - x_i(t)$.

As in the original paper [26] that introduced the Deffuant model, most later studies treated the initial opinions as independent and identically distributed according to the uniform distribution on the opinion space $[a, b]$. We also adopt this convention, as our goal is to explore the basic version of the Deffuant model in a systematic manner to provide a point of reference for results on the model’s variants. Nonuniform initial opinion distributions were considered, for example, in [62].

The confidence bound c characterizes a population’s tolerance of diverse viewpoints. If the opinion difference between a pair of agents is smaller than this threshold, they reduce their disagreement by making a compromise. Otherwise, the two agents keep their current opinions after they interact (or perhaps are unwilling to discuss the issue at all). In the extreme case of $c = 0$, no interaction can lead to compromise, and the initial opinion profile is a steady state. At the other extreme, if $c = b - a$, then with probability 1, any pair of interacting agents will compromise their opinions if they interact with each other. (In this case, the only situation without a compromise is

if one agent has an opinion of exactly a and the other has an opinion of exactly b .)

The multiplier (i.e., cautiousness parameter) m , which is called a *convergence parameter* in some papers [26,30,38,53], specifies a population’s cautiousness in the modification of opinions. A larger value of m indicates that individuals are more willing to compromise. In the special case $m = 0.5$, pairs of interacting agents agree on the mean of their opinions whenever their opinion difference is below the confidence bound. Prior studies of the Deffuant model typically have taken m between 0 and 0.5. However, we allow $m \in (0, 1)$, as taking $m > 0.5$ allows us to capture an “overadaptation” behavior. Overadaptive agents tend to comply with the beliefs of other agents, and they are sometimes seen as peacemakers [63–65]. Most past work has considered homogeneous m , but it would be interesting to examine the effects of heterogeneous levels of cautiousness. For example, [49] used a smooth influence function in which agents whose opinions have low uncertainty are more influential than those whose opinions have high uncertainty, and other types of heterogeneity are also worth exploring.

The Deffuant model, in its original form [26], considers the confidence bound and the multiplier to be constant in time and homogeneous across a whole population. In this setting, the mean opinion of two agents is the same before and after they interact.

Convergence of opinions is generally defined as the appearance of a stable configuration in which no more changes can occur. The steady-state opinion distribution is a superposition of Dirac delta functions in the opinion space $[a, b]$, such that consecutive spikes are separated by a distance of at least c . In other words, any two agents either hold the same opinion or their viewpoints differ by a distance of at least c . We use the notation $K \in \mathbb{N}$ to denote the number of steady-state opinion groups.

C. The Deffuant model on various networks

The agents in a Deffuant model are represented by nodes of a network, and a pair of agents on a randomly selected edge can interact with each other. To the best of our knowledge, the Deffuant model has been studied on only a few types of networks, including complete graphs, square lattices, Erdős–Rényi (ER) random graphs, Watts–Strogatz (WS) random graphs, and Barabási–Albert (BA) random graphs.

The Deffuant model on complete graphs has received considerable attention. Complete graphs can be used to model small communities, such as high-level political leaders in a country or inhabitants of a village, in which everyone knows each other. Complete graphs are also sometimes used as approximations for individual communities in large social networks, as individuals within communities are more closely connected with each other than with outsiders [66,67]. When there is homogeneous mixing in a population, the set of opinions always reaches a steady state [39]. It has been demonstrated numerically that a large confidence bound c yields consensus at steady state, whereas multiple opinion groups can persist for small values of c [26,30,38,40,41]. Such results were also obtained in simulations on square lattices, ER random graphs, WS random graphs, and BA random

graphs [16,26,45,68]. Moreover, some numerical simulations on complete graphs suggested that one can estimate the number K of major steady-state opinion groups by the integer part of $1/(2c)$ [26], such that perhaps the multiplier m and the number N of participating agents do not have a significant effect on K [26,30]. However, a later study [38] observed that the number of “major opinion” groups that include many agents is a function of c , and the number of “minor opinion” groups (i.e., groups of *minorities*) depends on m .

On square lattices, WS random graphs, and BA random graphs, the Deffuant model includes behavior that differs from that in homogeneously mixing populations. For instance, simulations on square lattices and BA random graphs suggest that K depends not only on c , but also on N , when multiple opinion groups persist at steady state [26,45]. Simulations on WS random graphs indicate that K depends both on c and on network architecture, and that the presence of “disorder” in the form of random “shortcut” edges seems to have only a small effect on the convergence time T [43].

Existing research on the Deffuant model on ER random graphs has often focused on adaptive networks, which evolve along with the opinions [16,68]. For WS random graphs, the study of the Deffuant model has centered around steady-state opinion groups [43].

III. METHODS

For each network structure, we conduct a regression analysis to examine convergence time as a function of confidence bound, the number of participating agents, and the multiplier that measures cautiousness. We then qualitatively examine the number of steady-state opinion groups.




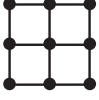

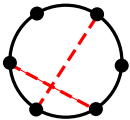
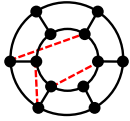
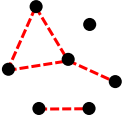
A. Networks studied

We study the Deffuant model on a variety of networks to improve understanding of the effect of network structure on convergence time and the number of steady-state opinion groups. Some of the networks that we study have deterministic structures, and others are random graphs. In Table I, we give notation, definitions, and examples for these networks. The first set of networks that we examine are deterministic graphs, including complete graphs (K_n), cycles (C_n), prism graphs (Y_n), square lattices (S_l), and complete multipartite graphs ($K_{n,r}$). These networks have been studied extensively because of their simple structures. Our simulation results on these networks provide reference points for comparisons with conclusions about (1) variants of the Deffuant model and (2) the original Deffuant model on more complicated network structures. The second set of networks that we study consists of random graphs: cycles with random edges ($C_{n,s}$) (which are related to WS small-world networks [71,72]), prism graphs with random edges ($Y_{n,s}$), and random graphs generated by the Erdős–Rényi $G(n, p)$ model. Finally, we investigate the Deffuant model on real social networks constructed using Facebook “friendship” data [58,59].

B. Simulation specifications

Without loss of generality, we consider the Deffuant model with opinions on the space $[0, 1]$ and the confidence bound

TABLE I. Summary of the definitions of the synthetic networks on which we study the Deffuant model. In each example network, solid lines represent deterministic edges, and dashed lines represent edges that are generated randomly.

Network	Definition	Example
K_n	A complete graph K_n has n pairwise adjacent nodes [61].	
C_n	For $n \geq 3$, a cycle C_n has node set $\{v_j \mid j \in \{1, \dots, n\}\}$ and edge set $\{v_j v_{j+1} \mid j \in \{1, \dots, n-1\}\} \cup \{v_n v_1\}$ [61].	
Y_n	For an even integer $n \geq 6$, let $\{v_j \mid j \in \{1, \dots, \frac{n}{2}\}\}$ and $\{w_j \mid j \in \{1, \dots, \frac{n}{2}\}\}$ be the node sets of two disjoint cycles. The prism Y_n is defined as the graph obtained by joining the two cycles using the edges $\{v_j w_j \mid j \in \{1, \dots, \frac{n}{2}\}\}$ [69].	
S_l	For a positive integer l , we define a square lattice S_l of side length l as the graph with node set $\{(x, y) \mid 0 \leq x, y \leq l, \text{ with } x, y \in \mathbb{Z}\}$ and edges $\{(x_1, y_1)(x_2, y_2)\}$ such that $\ (x_1 - x_2, y_1 - y_2)\ _2 = 1$.	
$K_{n,r}$	For an integer $r \geq 2$ and positive integers n_1, n_2, \dots, n_r , a complete r -partite graph K_{n_1, n_2, \dots, n_r} is a graph whose node set can be partitioned into r subsets (called partite sets) of sizes n_1, n_2, \dots, n_r , such that two nodes are adjacent if and only if they are from two distinct subsets. We consider complete r -partite graphs with equal-sized partite sets and denote such graphs as $K_{n,r}$, where r equals the number of partite sets and n (a multiple of r) is the size of the node set [70].	
$C_{n,s}$	For $n \geq 4$ and $s \in (0, \frac{n-3}{2})$, we define $C_{n,s}$ as follows: start with the cycle C_n and add edges uniformly at random between nonadjacent nodes until there are sn extra edges.	
$Y_{n,s}$	For an even integer $n \geq 6$ and $s \in (0, \frac{n-4}{2})$, we define $Y_{n,s}$ as follows: start with Y_n and add edges uniformly at random between nonadjacent nodes until there are sn extra edges.	
$G(n, p)$	For $n \in \mathbb{N}$ and $p \in [0, 1]$, we generate random graphs from the Erdős-Rényi (ER) $G(n, p)$ model [57] as follows: start with n disconnected nodes and place an edge between each distinct pair of nodes with independent probability p .	

$c \in [0, 1]$. In other words, we normalize the opinion dynamics so that each agent's opinion lies between 0 and 1 at each time step. We also consider the multiplier $m \in (0, 1)$, as opposed to the interval $(0, 0.5]$ in the original model [26]. This generalization is useful, as interacting agents can perhaps be convinced to believe in others' opinions more than their own. Moreover, considering $m \in (0, 1)$ reveals interesting phenomena that we will discuss in Sec. IV. A few of the parameter values have specific interpretations. For example, for $c = 1$, with probability 1, any pair of interacting agents makes convergent

opinion adjustments that correspond to interaction without a confidence bound. For $m = 0.5$, each pair of interacting agents agrees on their mean opinion whenever their opinion difference is below c . Theoretically, there is no upper bound on the number of agents that one can consider in a population, but running numerical simulations on extremely large populations is computationally intensive. For our simulations, we use a maximum of $N = 1000$ agents, and one can infer the behavior of the model for larger populations from our regression analyses.

The convergence time T and the number K of steady-state opinion groups are both difficult to predict, as the initial opinion profile, the pair of agents that interact at each time step, and the particular graphs generated by random-graph ensembles are all stochastic. To smooth out these sources of noise, we run 10 groups of independent simulations for each network in Sec. III A and each combination of the values of N , c , and m that we consider. During one simulation, we first generate a group of N independent and identically distributed initial opinions from a uniform distribution on $[0,1]$, and we then simulate the evolution of opinion dynamics according to the Deffuant model.

In principle, it takes infinitely long to reach a steady state, as the opinion space is continuous and opinions approach each other arbitrarily closely without reaching the same value in a finite time unless $m = 0.5$ [38]. However, the emergence of a steady state is evident at finite times, as consecutive opinion groups must be separated by a distance of at least c to avoid merging. Therefore, in practice, we need to set a convergence criterion in our numerical simulations. For our study, we consider an opinion profile to be a steady-state one if consecutive opinion groups are separated by a distance of at least c and the differences in each group are no more than 0.02. Based on some test runs, we also choose a bailout time of 10^9 iterations for each simulation. If a steady state is reached by the bailout time, we record the convergence time (T) and the number (K) of opinion groups. Otherwise, we record $T = 3.55 \times 10^9$, a strict upper bound that is higher than all possible convergence times, for the purpose of visualization.

IV. NUMERICAL SIMULATIONS AND RESULTS

In this section, we study the Deffuant model on various deterministic, randomly generated, and real-world networks by considering different network structures and interaction-parameter values. For each type of network, we first conduct data exploration and linear regression analysis to model convergence time (T) as a function of the number (N) of participating agents, the confidence bound (c), and the multiplier (m). We then discuss our qualitative observations about the number of steady-state opinion groups (K). In Appendix A 1, we provide a brief introduction to linear regression analysis. Because the processes of data exploration and regression analysis are

similar, we only give full details (in Appendix A 2) for a subset of the parameter space for our simulations on complete graphs.

We select the network structures that we present in this section based on features of the dynamics on them that we wish to highlight. We also study other examples, which we discuss in Appendix B. The examples that we relegate to Appendix B still have interesting dynamics, but similar dynamics arise in one or more of the examples in this section.

For each set of parameters and network structure that we consider, we conduct regression analysis using the mean results of 10 different simulations. We only use simulation results of networks with 100 or more agents to reduce the stochasticity introduced by the random initial opinion profile and to ensure that there is a sufficient quantity of data for testing the model assumptions. In Appendix C, we give detailed results of our statistical analysis for each of our examples.

A. Complete graphs

The simplest form of the Deffuant model allows any pair of agents in a system to interact [26]. This is equivalent to studying the model on a complete graph.

In Fig. 1, we summarize the values of $\ln(T)$ that we observe in simulations for various N (recall that N denotes the number of nodes in a graph), as these are representative of the trends that we observe in all simulations. We present a similar set of plots for other network structures in the subsequent subsections.

Our data exploration (see Appendix A 2) suggests that the convergence time T has qualitatively different behavior for $c < 0.5$ and $c \geq 0.5$, so we consider different regression models for these two cases.

For $c < 0.5$, model selection based on the Akaike information criterion (AIC) yields

$$\ln(\ln(T)) = \beta_0 + \beta_1 N + \beta_2 N^2 + \beta_3 c^2 + \beta_4 Nc + \epsilon, \quad (2)$$

where we assume that ϵ is an independent and normally distributed error with mean 0 and constant variance for every observation. We give our estimates for the coefficients β_j (with $j = 0, 1, \dots, 4$) in Table IV of Appendix C. The values of the AIC and R^2 are -2037.1 and 0.8246 , respectively.

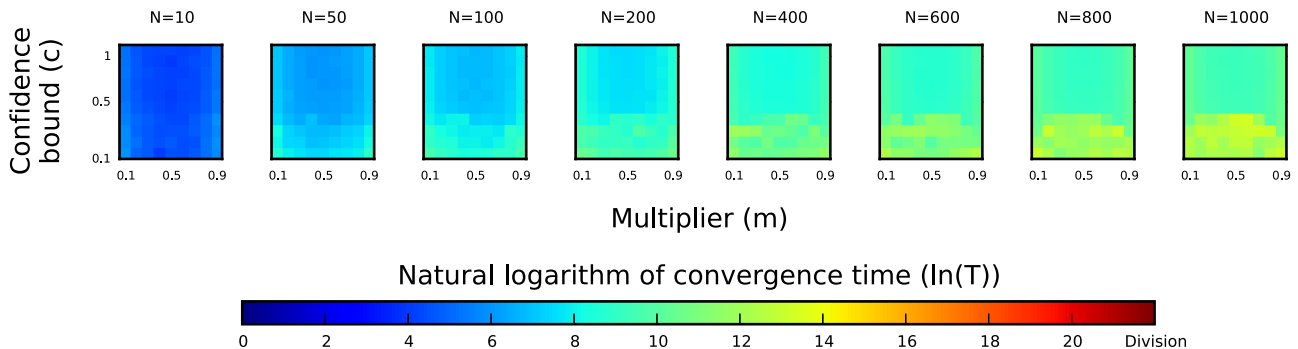


FIG. 1. Convergence times for simulations on N -node complete graphs for various N . These are representative of the trends that we observe in all simulations. (We generate this and all subsequent figures of this type using the MATPLOTLIB library for PYTHON developed by Hunter [73].)

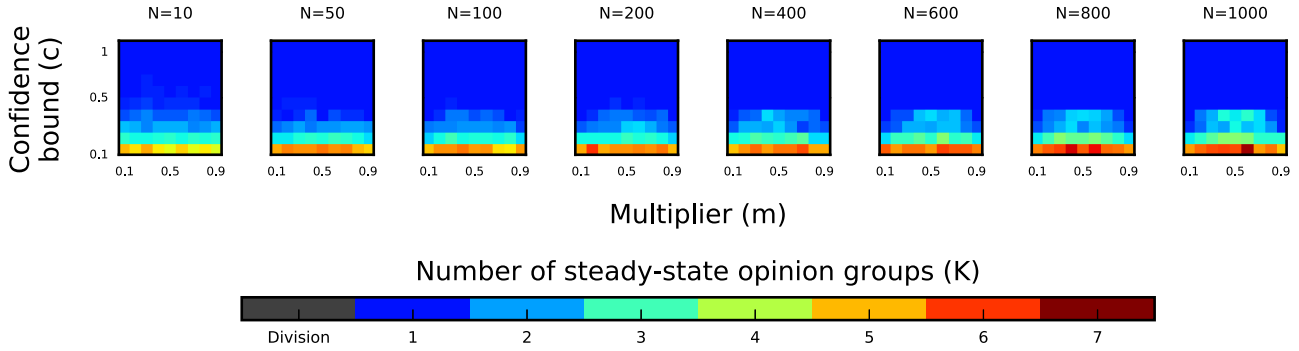


FIG. 2. Number of steady-state opinion groups in simulations on complete graphs for various N . These are representative of the trends that we observe in all simulations. We use the color gray to represent simulations that do not converge by the bailout time (10^9 iterations) in this figure and our subsequent figures of this type.

For $c \geq 0.5$, regression analysis suggests the model

$$\ln(T) = \beta_0 + \beta_1 \ln(N) + \beta_2(c - 1)^2 + \beta_3(m - 0.5)^2 + \epsilon, \tag{3}$$

where we give our estimates for the coefficients in Table V of Appendix C. The values of the AIC and R^2 are -3240.9 and 0.9964 , respectively.

The different forms of Eqs. (2) and (3) support our conjecture based on data exploration that T undergoes a transition at $c = 0.5$. More precisely, our regression results suggest that the behavior of T differs for $c \leq 0.4$ and $c \geq 0.5$. To determine a more precise transition point for c , one should conduct numerical simulations using $c \in (0.4, 0.5)$. For $c < 0.5$, the multiplier m has no statistically significant impact on T . Moreover, T tends to increase with N and tends to decrease with c . For $c \geq 0.5$, the effects of N , c , and m on T seem to be independent (or at least predominantly independent) of each other. In particular, T increases roughly linearly with N . We also observe that T increases exponentially with $(c - 1)^2$ and has a minimum at $c = 1$, which corresponds to interactions without a confidence bound. In other words, for fixed N and m , the convergence time on complete graphs is minimal when, with probability 1, any pair of interacting agents makes a convergent compromise. Our regression analysis also suggests that T increases exponentially with $(m - 0.5)^2$ and has a minimum at $m = 0.5$. This corresponds to the case in which each pair of interacting agents agrees at their mean opinion whenever their opinion difference is below the confidence bound.

For each combination of N , c , and m , we average the number K of steady-state opinion groups if and only if at least 60% of simulations reach steady state within the bailout time. Otherwise, we state that we observe a “division” of opinions for the associated parameter combination. We use the same standard to determine the number of steady-state opinion groups in our subsequent numerical experiments.

In Fig. 2, we summarize the number of steady-state opinion groups that persist in our simulations on complete graphs. We observe that K depends on N only when the confidence bound is $c < 0.5$, with the most dramatic changes occurring near $c = 0.1$. For $c \geq 0.5$, consensus is reached consistently. For $c \in [0.1, 0.4]$, we observe that K tends to increase with N . Additionally, for $c < 0.5$ and $N \geq 600$, we observe that K tends to be larger for m closer to 0.5. This is reasonable, because, as $m \rightarrow 0.5$, interacting agents tend to settle on the mean of their opinions, which reduces the length of time for opinions stabilize. Therefore, more opinion groups tend to persist at steady state.

B. Cycle graphs

In this subsection, we explore the behavior of the convergence time and the number of steady-state opinion groups by simulating the Deffuant model on N -node cycles. We will compare these simulation results to ones on cycles with additional, randomly placed “shortcut” edges in Sec. IV D.

In Fig. 3, we summarize the values of $\ln(T)$ that we observe in our simulations on cycles. Our simulations suggest that $\ln(T)$

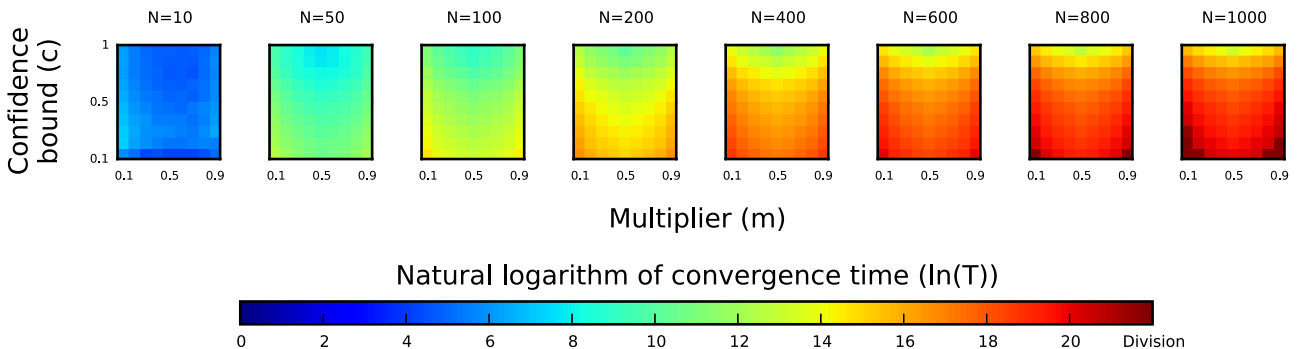


FIG. 3. Convergence time for simulations on N -node cycles for various N .

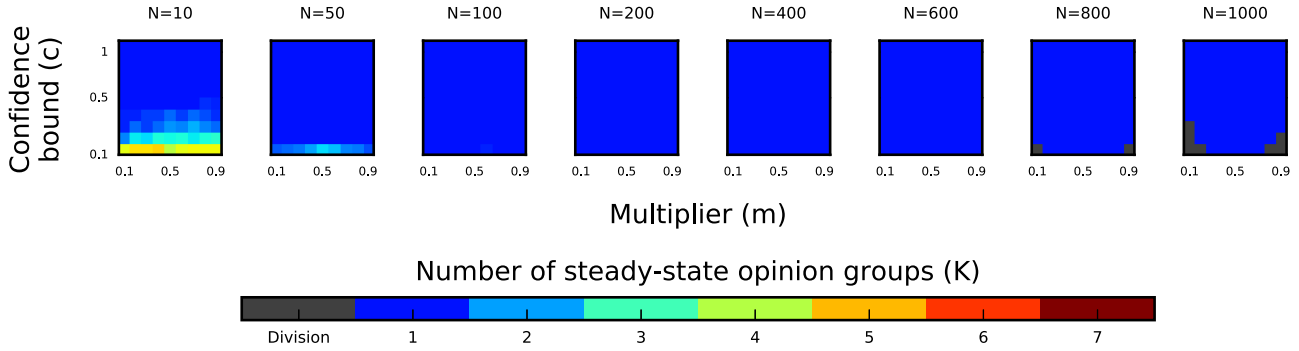


FIG. 4. Number of steady-state opinion groups in simulations on cycles for various N .

changes rapidly with m when c is close to 1. We speculate that a singularity arises at $c = 1$ and $m = 0.5$ as $N \rightarrow \infty$. Our linear regression models cannot capture singular points, and we exclude data points that correspond to $c \geq 0.7$ from our regression analysis for cycles. Our regression analysis gives the model

$$\ln(T) = \beta_0 + \beta_1 \ln(N) + \beta_2 c + \beta_3 c^2 + \beta_4 (m - 0.5)^2 + \beta_5 Nm + \epsilon, \quad (4)$$

where we give our coefficient estimates in Table VI of Appendix C. The values of the AIC and R^2 are -3257.6 and 0.9991 , respectively.

In contrast to our observations on complete graphs, our simulations on cycles indicate that the dependence of T on N , c , and m does not undergo a transition with respect to c . We observe that T decreases with c , and, as c gets closer to 1, the value of $\ln(T)$ changes with m increasingly rapidly as N increases. The convergence time T tends to increase with N and has a global minimum at approximately $m = 0.5$ for fixed values of N and c .

In Fig. 4, we summarize the number of steady-state opinion groups that arise in our simulations on cycles. A consensus is reached for $N \in [100, 700]$. Although some of our simulations for $N \in [800, 1000]$ do not converge by the bailout time, we conjecture that all simulations on cycles with large values of N will eventually converge, for any values of c and m , if the Deffuant dynamics occur for sufficiently many iterations. A consensus is reached when $c \geq 0.5$ for $N = 10$ and when $c \geq 0.2$ for $N = 50$. This observation is reasonable, as, with fewer agents, the initial opinions of neighboring nodes tend to

be farther apart, which leads to more groups. As with our results for complete graphs, we observe that more opinion groups tend to emerge in the final state as $m \rightarrow 0.5$ if multiple opinion groups persist at steady state.

C. Square lattice graphs

Apart from complete graphs, square lattices are the most common deterministic networks on which the Deffuant model has been studied previously [30]. In Fig. 5, we summarize the values of $\ln(T)$ that we observe in our simulations on square lattices. For $c < 0.5$, most of the simulations do not converge by the bailout time, so we conduct regression analysis for $c \geq 0.5$.

Our regression analysis suggests for $c \geq 0.5$ that

$$(\ln(T))^{1/4} = \beta_0 + \beta_1 \ln(N) + \beta_2 N + \beta_3 N^2 + \beta_4 c + \beta_5 c^2 + \beta_6 m + \beta_7 m^2 + \beta_8 Nm + \epsilon, \quad (5)$$

where we give our coefficient estimates in Table VII of Appendix C. The values of the AIC and R^2 are -5684.4 and 0.9908 , respectively. Equation (5) suggests that T increases with N and that T tends to decrease as c increases.

In Fig. 6, we summarize the number of steady-state opinion groups in our simulations on square lattices. As with our results on prism graphs (see Appendix B 1), a consensus occurs for all simulations on square lattices for $c \geq 0.5$.

D. Cycle graphs with random edges

We consider graphs generated by the ensemble $C_{N,s}$ (see Table I) for $s = 0.1$, $s = 0.2$, and $s = 0.3$. These cycles with

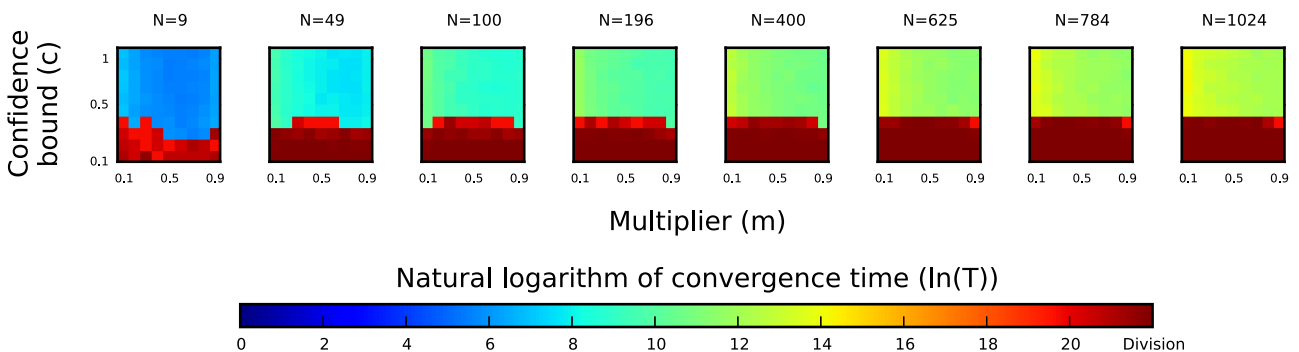


FIG. 5. Convergence times for simulations on square lattices.

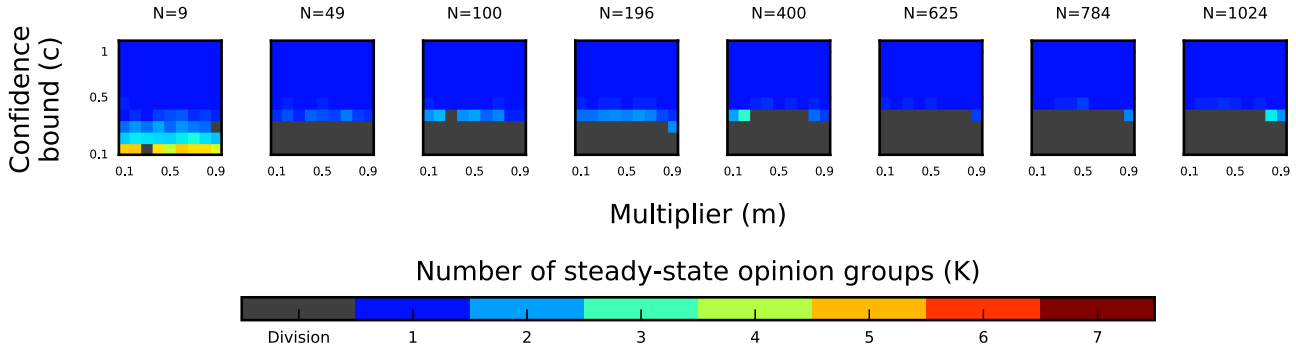


FIG. 6. Summary of the number of steady-state opinion groups in simulations on square lattices.

additional, random “shortcut” edges are related to Watts–Strogatz small-world networks [71,72,74] (see also earlier work by Bollobás and Chung [75]), except that nodes initially have degree 2, which yields (for cycles that are not too small) a clustering coefficient of 0 for each node before we add random edges.

In Fig. 7, we summarize the values of $\ln(T)$ that we observe in our simulations on $C_{N,s}$ for $s = 0.1$, $s = 0.2$, and $s = 0.3$. Regression analysis suggests the model

$$(\ln(T))^\alpha = \beta_0 + \beta_1 \ln(N) + \beta_2 N + \beta_3 N^2 + \beta_4 c + \beta_5 c^2 + \beta_6 (m - 0.5)^2 + \beta_7 Nc + \epsilon, \quad (6)$$

where the power-transformation parameter is $\alpha = -1/3$, $\alpha = -2/3$, and $\alpha = -5/6$ for $s = 0.1$, $s = 0.2$, and $s = 0.3$, respectively. For $s = 0.1$, the Nc term is statistically insignificant, so we drop it. In Table VIII of Appendix C, we summarize our coefficient estimates for Eq. (6). For $s = 0.1$, we obtain $AIC \approx -10378.2$ and $R^2 \approx 0.9853$; for $s = 0.2$, we obtain $AIC \approx -10443.3$ and $R^2 \approx 0.9829$; and for $s = 0.3$, we obtain $AIC \approx -10719.2$ and $R^2 \approx 0.9816$.

Our data exploration and regression analysis suggest that T does not experience a transition with respect to c . According

to Eq. (6), T increases with N for $s = 0.1$, $s = 0.2$, and $s = 0.3$. Additionally, T has a global minimum at $m = 0.5$ for fixed N and c . Adding random shortcut edges to cycles significantly decreases the convergence time. Additionally, T increases much more slowly with N for $C_{N,s}$ graphs than it does for cycles.

In Fig. 8, we summarize the number of steady-state opinion groups in our simulations on cycles with random edges. With only a small proportion (specifically, $s = 0.1$) of random edges, the number K of steady-state opinion groups is roughly the same as what we observed in our simulations on cycles (see Fig. 4). However, with progressively more random edges, multiple opinion groups start to emerge at steady state for $c \leq 0.3$. We conjecture that, as we increase the fraction of random edges relative to deterministic ones, the behavior of K becomes progressively more similar to complete graphs than to cycles.

E. Erdős–Rényi graphs

We now consider random graphs generated by the Erdős–Rényi $G(N, p)$ model, where $p \in [0, 1]$ is an independent probability for an edge to exist between a pair of nodes.

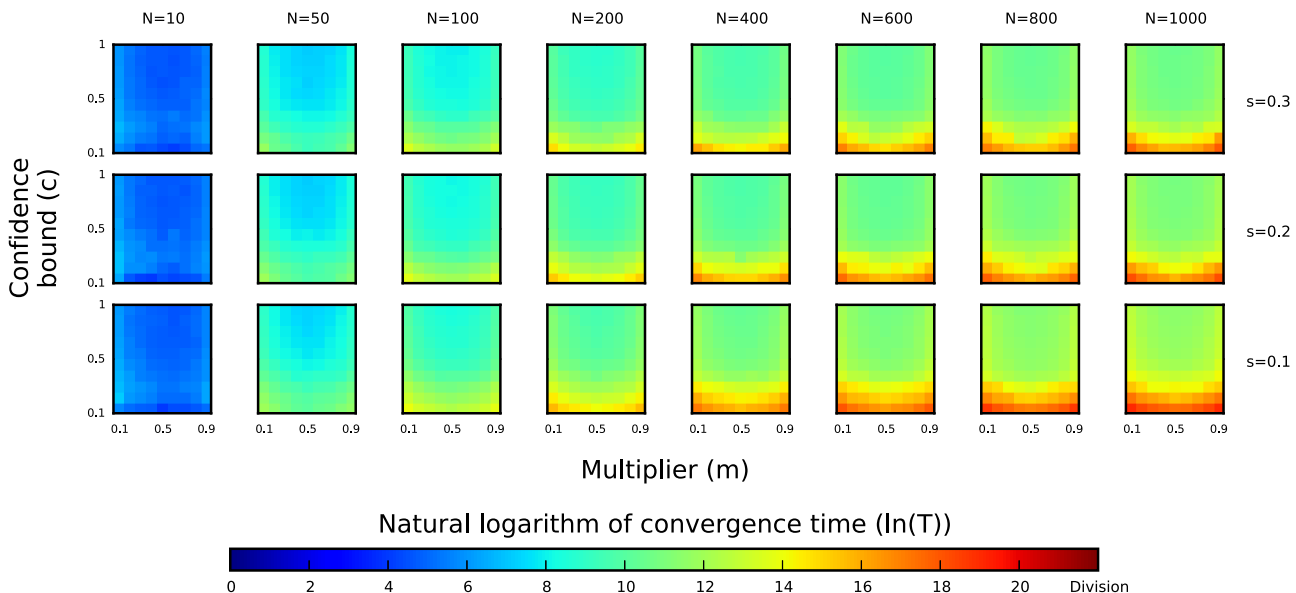


FIG. 7. Convergence times for simulations on $C_{N,s}$ for $s = 0.1$, $s = 0.2$, and $s = 0.3$ for various values of N .

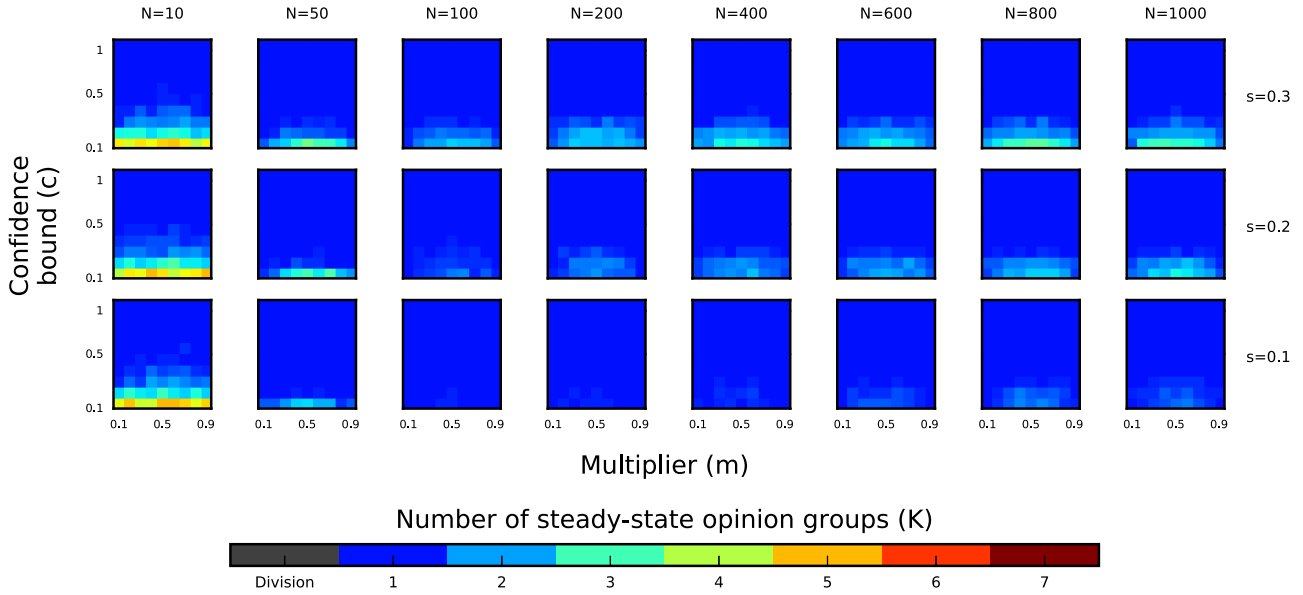


FIG. 8. Number of steady-state opinion groups in simulations on $C_{N,s}$ for $s = 0.1, s = 0.2,$ and $s = 0.3$ for various values of N .

Erdős–Rényi graphs are one of the best-studied random-graph models [42], and they have been used in previous studies of the Deffuant model on networks [16,41,68,76]. Interestingly, existing research on the Deffuant model on ER random graphs has often focused on adaptive networks that evolve along with the opinions [16,68]. In our simulations, we consider the ER $G(N, p)$ model for $p = 0.1, 0.2, \dots, 0.9$. Complete graphs are a special case of the ER $G(N, p)$ model, as one obtains a complete graph for $p = 1$.

In Fig. 9, we show a subset of the values of $\ln(T)$ that we obtain in our simulations. These values are representative of the observed trends in all of our simulations. As in our simulations on complete graphs, we observe qualitatively distinct behavior for T for $c < 0.5$ and $c \geq 0.5$. Therefore, we conduct separate

regression analyses for these two cases. For $c < 0.5$, our regression analysis suggests the model

$$\ln(\ln(T)) = \beta_0 + \beta_1 N + \beta_2 N^2 + \beta_3 c^2 + \beta_4 (m - 0.5)^2 + \beta_5 Nc + \epsilon, \tag{7}$$

where we give estimates for the coefficients in Table IX. Random graphs generated by the ER $G(N, p)$ model are a source of stochasticity for the opinion dynamics. It is thus not surprising that we observe a larger number of outliers for our ER simulations than for complete graphs. Let $q \in [0, 1]$ be the proportion of data points that we identify as outliers and thus exclude from our regression analysis. (We construe a data point as an outlier if $T > 600\,000$. Each data point

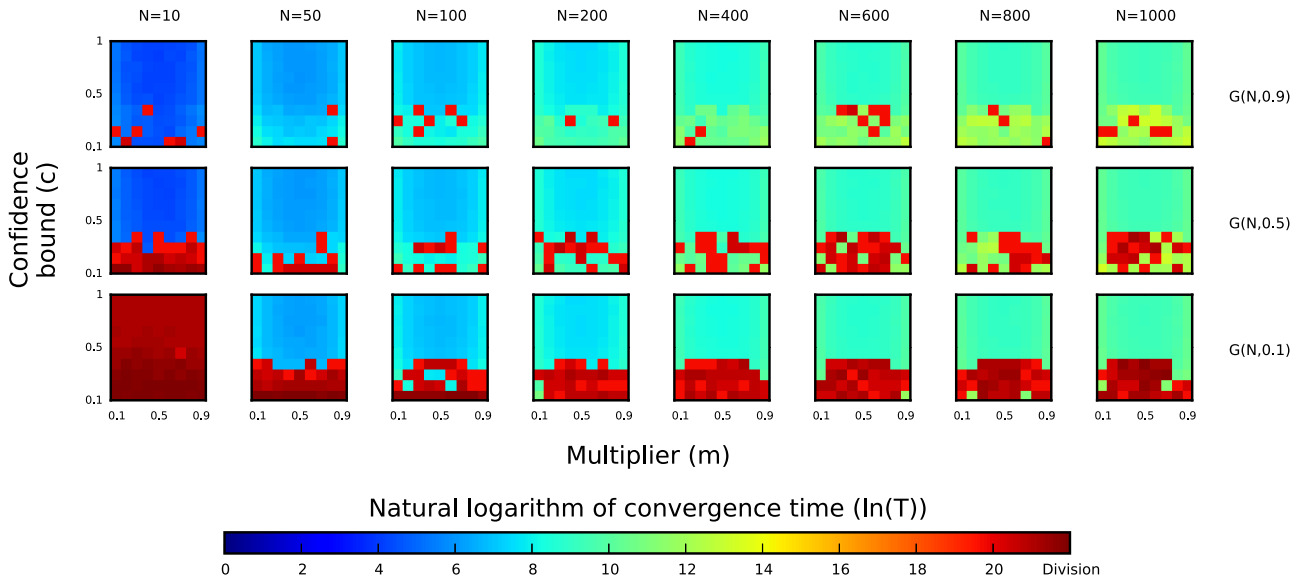


FIG. 9. Convergence times for simulations on random graphs generated by the Erdős–Rényi $G(N, p)$ model. We conduct simulations for $p = 0.1, 0.2, \dots, 0.9$, and we present a subset of our plots to illustrate the observed trends.

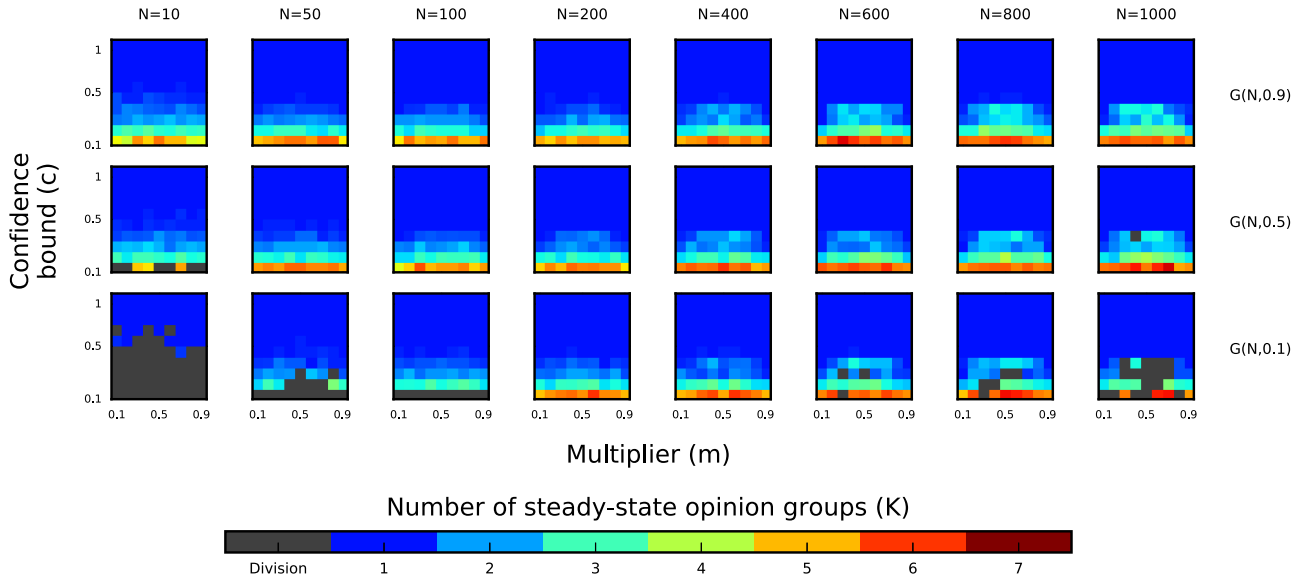


FIG. 10. Number of steady-state opinion groups in simulations on random graphs generated by the Erdős–Rényi $G(N, p)$ model. We conduct simulations for $p = 0.1, 0.2, \dots, 0.9$, and we present a subset of our plots to illustrate the observed trends.

is a mean over 10 simulations, and we choose this value of T so that all 10 simulations converge by the bailout time of 3.55×10^9 .) For $c < 0.5$, we conduct a regression analysis for the $G(N, p)$ graphs for $p = 0.7, p = 0.8$, and $p = 0.9$, as $q > 0.15$ for smaller values of p (and this would undermine the reliability of the regression analysis). For $p = 0.7$, we obtain $q \approx 0.1133$, $AIC \approx -1515.5$, and $R^2 \approx 0.8360$; for $p = 0.8$, we obtain $q \approx 0.0767$, $AIC \approx -1658.1$, and $R^2 \approx 0.8114$; and for $p = 0.9$, we obtain $q = 0.05$, $AIC \approx -1774.1$, and $R^2 \approx 0.7984$. For $c \geq 0.5$, our regression analysis suggests the model in Eq. (3) for each value of p that we consider. For each p , Table X of Appendix C gives our estimates for the coefficients β_j (with $j = 0, 1, 2, 3$), together with the corresponding values of AIC and R^2 .

The different forms of Eqs. (3) and (7) support our conjecture from our data exploration that T undergoes a transition at $c = 0.5$. For $c < 0.5$, the convergence time T tends to increase with N and tends to decrease with c . Equation (7) suggests that $\ln(T)$ is proportional to $\exp[(m - 0.5)^2]$ for $c < 0.5$, in contrast to the results of our regression model for complete graphs [see Eq. (2)], which does not illustrate a statistically significant influence of m on T . For $c \geq 0.5$, our regression model for the ER $G(N, p)$ model is the same as what we obtained for complete graphs, so the behavior of T with respect to N, c , and m is similar in that parameter regime. For large values of p , the estimated coefficients are very close to those for complete graphs. This suggests that it is probably accurate to use a mean-field approximation to study convergence time for the Deffuant model on Erdős–Rényi $G(N, p)$ graphs if p is close to 1.

In Fig. 10, we illustrate the number of steady-state opinion groups that arise in our simulations of the Deffuant model on random graphs generated by the ER $G(N, p)$ model. When the connection probability p is close to 1, the behavior of K is similar to what we observed for complete graphs. As $p \rightarrow 0$, the major qualitative difference is that opinions sometimes

fail to converge within the bailout time for small values of c . This is reasonable, because random graphs generated by the ER $G(N, p)$ model with small p values normally have small components in addition to the largest connected component. This impedes (and can also prevent) convergence of opinions.

V. CONCLUSIONS AND DISCUSSION

We studied the Deffuant model on several types of deterministic and random networks. For each of these networks, we systematically examined the number of groups of different opinions and the time to reach steady state as a function of the number (N) of agents that participate in the opinion dynamics, the population’s confidence bound (c), and their cautiousness (which we measure using the multiplier m). For the time to reach steady state, we used both numerical simulations and regression analyses to obtain qualitative and quantitative insights. For the number K of steady-state opinion groups, we used numerical simulations to examine the qualitative behavior of the dynamics in different types of networks.

We obtained many insights from our systematic computations. Studying the effects of network structure on dynamical processes (such as opinion models) is challenging, and we were able to achieve several interesting insights about the intertwined effects of network topology and the parameter values of the Deffuant model on the convergence time T . For example, our regression analyses suggest that the convergence time T undergoes a transition at a critical value of the confidence bound ($c = 0.5$) on complete graphs, prism graphs, prism graphs with random edges, and Erdős–Rényi networks, but not on cycles or cycles with random edges. For the prism and cycle examples, it is interesting that adding a small number of edges uniformly at random does not seem to alter the presence or absence of a transition in T . We observed some dynamical features only in specific types of networks. For complete

graphs, m has no statistically significant effect on T for $c < 0.5$, whereas T increases exponentially with $(m - 0.5)^2$ for $c \geq 0.5$. For cycles, we speculated based on simulation results that T has a singularity at $c = 1$ and $m = 0.5$ as $N \rightarrow \infty$. Another interesting observation is that our ER graphs, ranging from very sparse graphs to complete graphs, have a very similar relationship (for all values of p that we considered) between T and the other parameters for $c \geq 0.5$. This suggests that it would be useful to study the Deffuant model on ER graphs using a mean-field approximation, especially as useful results have been obtained for other dynamical processes in this way [13]. Additionally, adding random shortcut edges to cycles and prism graphs significantly decreases the convergence time, especially for small values of c . For all networks, our regression analyses suggest that T tends to decrease as c increases and that T tends to increase as N increases.

Our results also shed further light on educated guesses and other claims that have appeared in the literature. We examined quantitatively how the convergence time T increases with the number N of agents in a network, and we thereby obtained several insights for Deffuant dynamics on different network topologies. For example, although [38] speculated that T is proportional to N , our regression results indicate that the linear relationship need not hold and that it depends on the underlying network topology. Additionally, several papers have concluded based on numerical simulations for a few values of the multiplier m that consensus occurs for the Deffuant model for several networks (e.g., ER networks, WS networks, and BA networks) when the confidence bound is large, whereas multiple opinion groups persist at steady state for low confidence bounds [30,38,40,41]. However, different transition thresholds (e.g., 0.25, 0.3, and 0.5) have been proposed for the confidence bound c . In the synthetic networks that we study (except for cycles and cycles with random edges), our simulation results suggest that a transition threshold of $c \in [0.4, 0.5]$ is most likely for large populations. For $c \geq 0.5$, consensus occurs on all of our families of deterministic networks (both synthetic and empirical), except for bipartite graphs. For $c < 0.5$, more opinion groups persist at steady state as node degree increases for our simulations on k -regular graphs given by cycles (for which the degree is $k = 2$ for each node), prism graphs ($k = 3$ for each node), and complete graphs (of progressively larger size, starting from $N = 10$ nodes, and hence of progressively larger degree for each node). This is possibly because, with larger k , agents in a k -regular graph have more neighbors with “competing” opinions, which makes it harder for them to make up their minds. Therefore, more opinion groups remain at steady state. Additionally, it was proposed in [26] based on numerical simulations that one can approximate the number of major steady-state opinion groups by the integer part of $1/(2c)$ for a large population. However, our simulations show that this statement is not true in general. For instance, for simulations on prism graphs, $K = 2$ for $c \geq 0.3$ when N is large.

Our simulations suggest that the number K of steady-state opinion groups is similar for random-graph models and appropriate counterpart deterministic networks (at least for the network families that we study). For example, adding a small number of uniformly random edges per node (specifically, the number of random edges divided by total number of nodes is small) to cycles and prism graphs does not have an obvious

impact on K . We conjecture that K approaches the value that one obtains for complete graphs as one progressively increases the proportion of random edges relative to deterministic ones on cycles and prism graphs. For the Erdős–Rényi $G(N, p)$ model, we observed that the behavior of K is similar to that on complete graphs when the edge generation probability p is close to 1, corroborating the potential usefulness of a mean-field approximation.

Our results provide insight into the convergence of opinion dynamics into stable groups of different opinions and on how long it takes to achieve such groups in differently structured populations. For instance, when it is desirable to achieve a consensus among many individuals (especially in a potentially contentious situation), one may try to obtain agreement as quickly as possible, and it is useful to obtain a better understanding of which network structures can best achieve such useful outcomes. It is also noteworthy that one topic in early studies of bounded-confidence models such as the Deffuant model was to examine how extremism can take hold in a population [48,49,77], and (perhaps especially given recent events) it seems useful to revisit such applications of these models. In developing models further for such applications, it will be important to incorporate recent insights, such as those in [9].

Our systematic approach for studying the Deffuant model on various network structures is also applicable to other bounded-confidence models and to models of opinion dynamics more generally. For example, the Hegselmann–Krause model was invented and subsequently attracted much attention at about the same time as the Deffuant model. It would be interesting to study the HK model using a systematic approach that is similar to the one in the present paper. One can also generalize bounded-confidence models to incorporate population heterogeneity, such as by drawing cautiousness parameters from a distribution (analogous to what is done in threshold models of social influence [13,78]), rather than using the same value for all individuals, as openness to compromise varies among individuals. Another generalization is to take background social conditions into account, such as by allowing agents’ interactions to have divisive effects [79,80]. Distinguishing major and minor opinion groups is also an important future direction for systematic studies of opinion-dynamics models. Our regression approach should also be useful more generally for studying dynamical processes on networks, including generalizations of standard graph structures (such as multilayer networks [81], temporal networks [82], and adaptive networks [83]).

ACKNOWLEDGMENTS

We thank Mariano Beguerisse Díaz, Jean-Philippe Bouchaud, and the anonymous referees for helpful comments.

APPENDIX A: STATISTICAL ANALYSIS

In this appendix, we illustrate our statistical analysis in detail. For concreteness, we briefly introduce linear regression in Sec. A1, and we then discuss our analysis in the context of the Deffuant model on complete graphs in Sec. A2. We perform the same procedure for all of our regression analyses.

1. Linear regression models

In this subsection, we provide a brief introduction, based on the one in [84], to linear regression models. A key benefit of a regression approach is that it permits one to draw far more accurate inferences with small sample sizes than one can obtain using data fitting.

Given a data set $\{(x_i, y_i)\}$ for which the scalar y_i is a dependent variable and the vector x_i denotes the explanatory variables, a linear regression model takes the form

$$y_i = \hat{y}(x_i, \beta) + \epsilon_i \quad \text{for all } i, \tag{A1}$$

$$\hat{y}(x_i, \beta) = \beta_0 + \beta_1 \Phi_1(x_i) + \dots + \beta_l \Phi_l(x_i), \tag{A2}$$

where ϵ_i is a mean-0 noise term and Φ_j are basis functions that extract important features of the explanatory variables. The model is linear in the unknown parameters β_j , which one estimates from data. Linearity allows the model to have simple analytical properties. Nevertheless, linear regression models are powerful tools for describing the relationship between the dependent variable and the explanatory variables, as Φ_j can have nonlinear forms.

We fit Eq. (A1) to $\{(x_i, y_i)\}$ by minimizing a sum-of-squares error function $\sum_i [\hat{y}(x_i, \beta) - y_i]^2$ over β . For this loss function, the estimator is unbiased and consistent if ϵ_i have the same finite variance and are uncorrelated with x [85]. If it is also the case that ϵ_i are normally distributed, then Eq. (A2) is also the maximum-likelihood estimator. We evaluate these assumptions throughout our model-selection process.

For model selection, we use the Akaike information criterion (AIC) [86] to select the “best” subset of basis functions, as this method balances the trade-off between the goodness of fit and the complexity of a model. This model-selection approach aims to minimize the AIC value

$$\text{AIC} = 2[k - \ln(L)], \tag{A3}$$

where k is the number of estimated parameters and L is the maximum value of the likelihood function for the model. The “coefficient of determination” $R^2 \in [0, 1]$ measures the fraction of variation in the data that is explained by a regression model, with $R^2 = 0$ implying no fit and $R^2 = 1$ implying a perfect fit. The formula for the coefficient of determination is

$$R^2 = 1 - \frac{\sum_i [y_i - \hat{y}(x_i, \beta)]^2}{\sum_i (y_i - \bar{y})^2}, \tag{A4}$$

where \bar{y} is the sample mean. We use the AIC to select regression models and R^2 to measure the goodness of fit.

2. Statistical analysis of simulation results on complete graphs

The scatter plots in Fig. 11 suggest that the convergence time (T) depends on the number (N) of participating agents, the population’s confidence bound (c), and possibly on their cautiousness (which we measure using the multiplier m). In particular, the relationship between T and c seems to undergo a transition at a critical value $c = 0.5$, below which we observe a larger variation in T . In Fig. 12, we show separate scatter plots for $c < 0.5$ and $c \geq 0.5$ to illustrate the qualitatively distinct behavior in the two regimes.

First, we consider the case $c < 0.5$. We start by fitting a linear model

$$T = \beta_0 + \beta_1 N + \beta_2 N^2 + \beta_3 c + \beta_4 c^2 + \beta_5 m + \beta_6 m^2 + \beta_7 mc + \beta_8 Nc + \beta_9 Nm + \epsilon, \tag{A5}$$

where β_j (with $j = 0, 1, \dots, 9$) are coefficients to be estimated and we assume for each observation that ϵ is an independent and normally-distributed error with mean 0 and constant variance. To account for the curvature observed in Fig. 12, we include explanatory variables up to second order in the model in Eq. (A5). We will subsequently drop statistically insignificant variables in a model-reduction procedure.

Before proceeding with model selection, we check the validity of our model assumptions. In Fig. 13, we check the assumption that the errors have mean 0 and constant variance by plotting studentized residuals versus the response values predicted by Eq. (A5). Ideally, variance should be constant in the vertical direction, and the scatter should be symmetric vertically about 0. However, Fig. 13 indicates that the variance is not constant, as the points follow a clear wedge-shaped pattern, with the vertical spread of the points increasing with the fitted values. In Fig. 13, we check the assumption of normality by plotting the sample quantiles versus the quantiles of a normal distribution. Data generated from a normal distribution should closely follow the 45° line through the origin, but this is contradicted by the $Q-Q$ plot in Fig. 13. Therefore, the diagnostics show the necessity of stabilizing the variance to make the data more like a normal distribution.

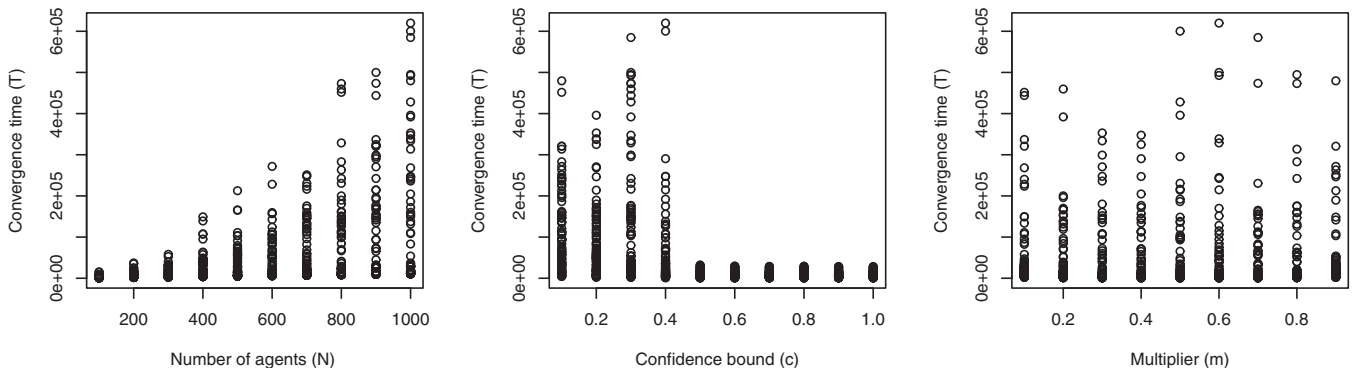


FIG. 11. Scatter plots of convergence time (T) on complete graphs versus the number of agents (N), the confidence bound (c), and the multiplier (m). (We drew this figure using the software environment R [87].)

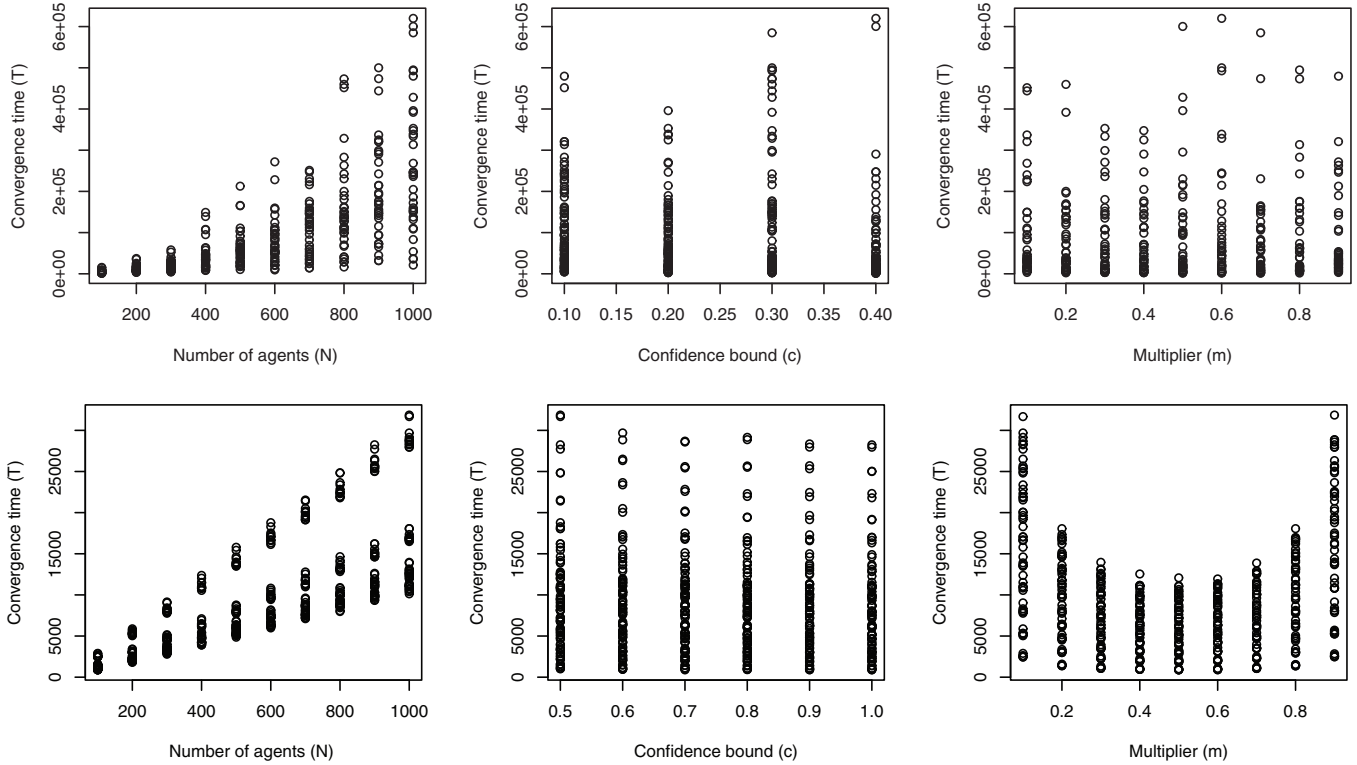


FIG. 12. Scatter plots of T versus N , c , and m using simulation results on complete graphs with confidence bound (top) $c < 0.5$ and (bottom) $c \geq 0.5$. (We drew this figure using R [87].)

The one-parameter Box–Cox method [88] is a popular way to determine a transformation on strictly positive scalar dependent variables (which are sometimes known as “responses” in this context) [89]. A Box–Cox transformation maps T to $T^{(\lambda)}$, where the family of transformations indexed by $\lambda \in \mathbb{R}$ is defined by

$$T^{(\lambda)} = \begin{cases} \frac{T^\lambda - 1}{\lambda}, & \text{if } \lambda \neq 0, \\ \ln(T), & \text{if } \lambda = 0. \end{cases} \quad (\text{A6})$$

In Fig. 14, we show that the confidence interval for λ at the 95% confidence level is roughly $[-0.2, 0]$. We choose to

set $\lambda = 0$, as this corresponds to taking a natural logarithm. The diagnostics of the new model suggest another logarithmic transformation, leading to the model

$$\begin{aligned} \ln(\ln(T)) = & \beta_0 + \beta_1 N + \beta_2 N^2 + \beta_3 c + \beta_4 c^2 + \beta_5 m \\ & + \beta_6 m^2 + \beta_7 mc + \beta_8 Nc + \beta_9 Nm + \epsilon, \end{aligned} \quad (\text{A7})$$

where we assume for each observation that ϵ is an independent and normally-distributed error with mean 0 and constant variance. The variance for ϵ is not necessarily the same for

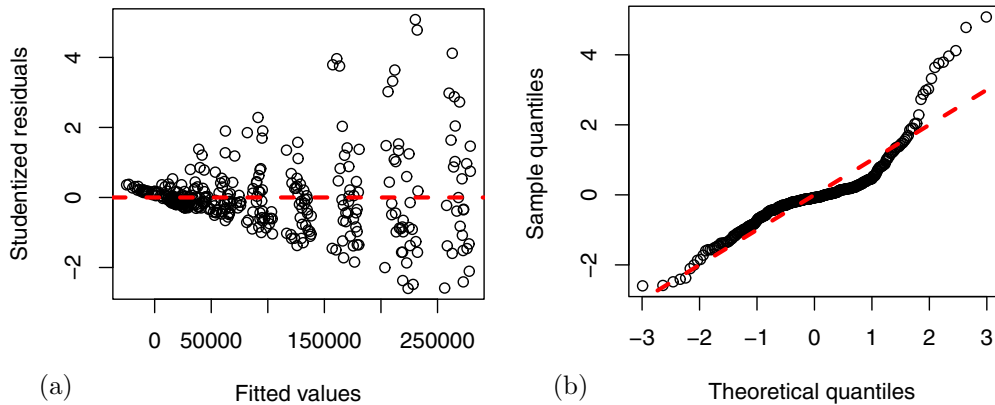


FIG. 13. (a) Studentized residuals versus fitted values and (b) normal Q – Q plot of studentized residuals for Eq. (A5) using our simulation results on complete graphs with confidence bound $c < 0.5$. In panel (a), the dashed reference line is the horizontal line through the origin. Ideally, variance should be constant in the vertical direction, and the scatter should be symmetric vertically about 0. In panel (b), the dashed reference line is the 45° line through the origin. Data generated from a normal distribution should closely follow the dashed line.

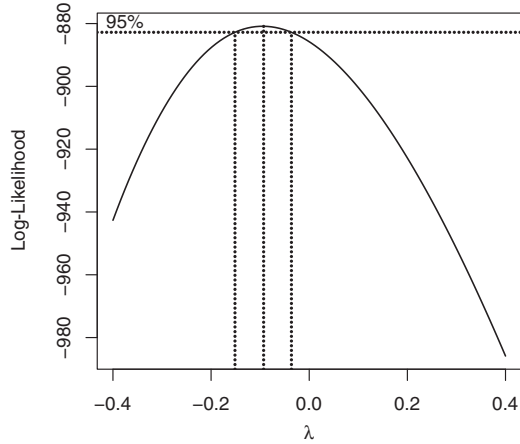


FIG. 14. Profile log-likelihood for the parameter λ of the Box–Cox transformation.

Eqs. (A5) and (A7). However, we use the same notation for ϵ , with the understanding that it is of course allowed to be different for different models.

We again evaluate our assumptions, and we show our results in Fig. 15. This time, we observe approximately constant variance in the vertical direction, and the scatter is roughly symmetric vertically about 0. There are no studentized residuals outside the $[-3, 3]$ range, revealing no serious outliers. In Fig. 15, the points closely follow the 45° line through the origin. Therefore, our model assumptions appear to be reasonable for Eq. (A7).

It is also important to minimize the number of regression terms in our models. Based on the results of AIC-based model selection, we drop the linear term in c that is independent of N and all terms that include m to yield Eq. (2). The diagnostic graphs for Eq. (2) are similar to those in Fig. 15 and are therefore acceptable.

Cook’s distance [90] measures the influence of a data point in a least-squares regression analysis. A common threshold for detecting highly influential observations is $8/(\bar{n} - 2\bar{k})$, where \bar{n} is the number of observations and \bar{k} is the number of fitting

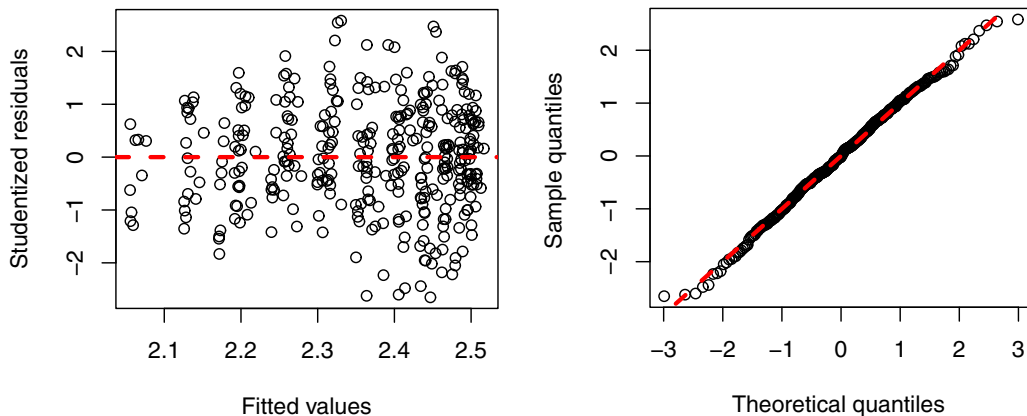


FIG. 15. (a) Studentized residuals versus fitted values and (b) normal $Q-Q$ plot of studentized residuals for Eq. (A7) using simulation results on complete graphs with confidence bound $c < 0.5$. The dashed reference lines in panels (a) and (b) are, respectively, the horizontal line through the origin and the 45° line through the origin. These diagnostic plots show that our model assumptions of normally-distributed errors with mean 0 and constant variance are reasonable for Eq. (A7).

TABLE II. Values of AIC and R^2 of regression models that we consider for our simulations on complete graphs with confidence bound $c < 0.5$. They are accurate to 5 and 4 significant figures, respectively.

Model	AIC	R^2
Eq. (A5)	8148.1	0.5272
Eq. (A7)	-2038.5	0.8164
Eq. (2)	-2044.9	0.8246

parameters. Figure 16 reveals 3 highly influential observations (which are very far above the threshold) for the model given by Eq. (2). We remove these 3 points and give the resulting estimates (accurate to 4 significant figures) for the coefficients β_j (with $j = 0, 1, \dots, 4$) of Eq. (2) in Table IV of Appendix C.

In Table II, we summarize the values of AIC and R^2 for the regression models that we consider for simulations on complete graphs with confidence bound $c < 0.5$. The substantial increase in R^2 and decrease in AIC indicate that our final model [see Eq. (2)] has a much better goodness of fit and a considerably simpler form than our original model [see Eq. (A5)].

For $c \geq 0.5$, we go through a model-selection process similar to that for $c < 0.5$, and we obtain

$$\ln(T) = \beta_0 + \beta_1 \ln(N) + \beta_2 c + \beta_3 c^2 + \beta_4 m + \beta_5 m^2 + \epsilon. \tag{A8}$$

We include an $\ln(N)$ term in the full model [see Eq. (A8)] to account for the linear dependence of T on N that Fig. 12 suggests. AIC-based model selection indicates the statistical significance of the $\ln(N)$ term. For Eq. (A8), we obtain $\text{AIC} \approx -3248.9$ and $R^2 \approx 0.9965$. In Table III, we give our estimates for the coefficients β_j (with $j = 0, 1, \dots, 5$) of Eq. (A8).

Table III suggests that one should combine m and m^2 into a single term $(m - 0.5)^2$, and it also suggests that one should combine c and c^2 into $(c - 1)^2$. The model with the combined terms has $\text{AIC} \approx -3240.9$ and $R^2 \approx 0.9964$, which are very close to those of Eq. (A8) but with two fewer coefficients

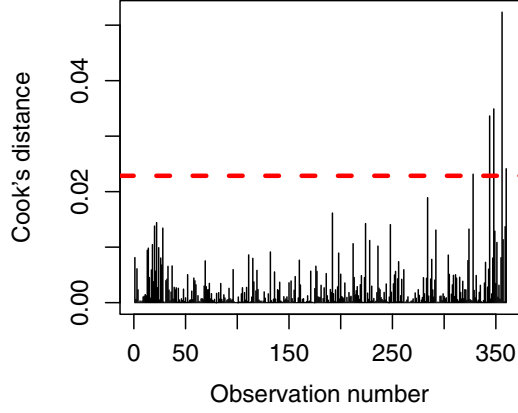


FIG. 16. Cook's distances for the regression model in Eq. (2). The dashed line is a horizontal line through $8/(\bar{n} - 2\bar{p})$, where \bar{n} is the number of observations and \bar{p} is the number of fitting parameters. This line gives the threshold for detecting highly influential observations that are particularly worth checking for validity.

to estimate. Therefore, we update our model for $c \geq 0.5$ to the simpler model in Eq. (3). We give our estimates for the coefficients of Eq. (3) in Table V of Appendix C.

APPENDIX B: ADDITIONAL EXAMPLES

1. Prism graphs

In this subsection, we explore the behavior of convergence time and the number of steady-state opinion groups by simulating the Deffuant model on prism graphs (which are a special type of generalized Petersen graph [91]). We will compare our simulation results on prism graphs to those on prisms with additional random edges in Sec. B 3.

In Fig. 17, we summarize the values of $\ln(T)$ that we observe in our simulations on prism graphs. As with our computations for complete graphs in Sec. IV A, scatter plots of $\ln(T)$ versus N , c , and m exhibit qualitatively distinct behavior for $c < 0.5$ and $c \geq 0.5$. We thus conduct separate regression analyses for $c < 0.5$ and $c \geq 0.5$. For $c < 0.5$, regression analysis suggests the model

$$(\ln(T))^2 = \beta_0 + \beta_1 N + \beta_2 N^2 + \beta_3 c + \beta_4 c^2 + \beta_5 (m - 0.5)^2 + \beta_6 Nc + \epsilon, \quad (\text{B1})$$

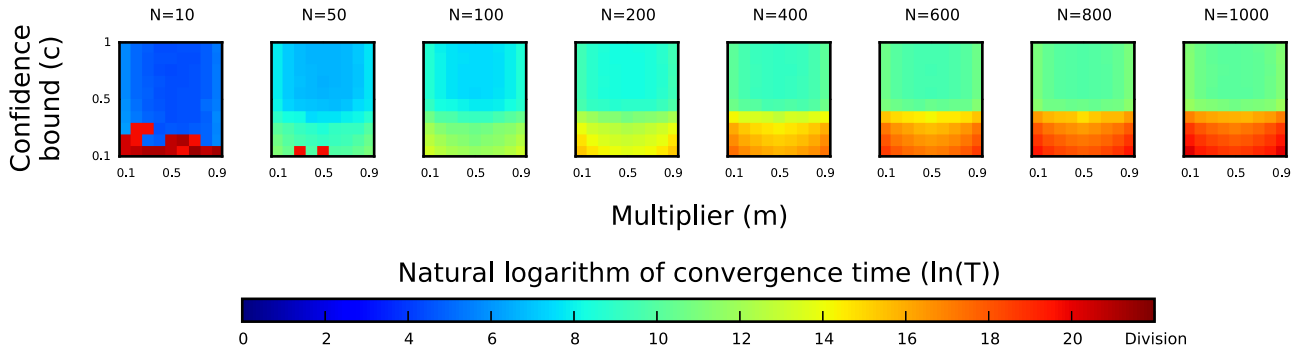


FIG. 17. Convergence times for simulations on N -node prism graphs for various N .

TABLE III. Estimates of regression parameters for Eq. (A8).

	Estimate	Std. Error	t value	$\text{Pr}(> t)$
β_0	4.024	5.038×10^{-2}	7.988×10	$< 2 \times 10^{-16}$
β_1	1.062	3.039×10^{-3}	3.495×10^2	$< 2 \times 10^{-16}$
β_2	-1.316	1.277×10^{-1}	-1.031×10	$< 2 \times 10^{-16}$
β_3	7.346×10^{-1}	8.472×10^{-2}	8.671	$< 2 \times 10^{-16}$
β_4	-6.261	3.704×10^{-2}	-1.690×10^2	$< 2 \times 10^{-16}$
β_5	6.262	3.612×10^{-2}	1.733×10^2	$< 2 \times 10^{-16}$

where we give our coefficient estimates in Table XI of Appendix C. The values of the AIC and R^2 are 1301.9 and 0.9919, respectively. For $c \geq 0.5$, regression analysis suggests the model

$$\sqrt{\ln(T)} = \beta_0 + \beta_1 \ln(N) + \beta_2 c + \beta_3 c^2 + \beta_4 (m - 0.5)^2 + \beta_5 Nc + \epsilon, \quad (\text{B2})$$

where we give our coefficient estimates in Table XII of Appendix C. The values of the AIC and R^2 are -4219.1 and 0.9845, respectively.

As with complete graphs, the different forms of Eqs. (B1) and (B2) support our conjecture based on data exploration that T undergoes a transition at $c = 0.5$. According to Eqs. (B1) and (B2), T tends to increase with N . Additionally, T increases with respect to N more rapidly for $c < 0.5$ than for $c \geq 0.5$. The convergence time T tends to decrease as c increases for fixed values of N and m . The convergence time T has a global minimum at $m = 0.5$ for constant N and c .

In Fig. 18, we summarize the number of opinion groups that persist in our simulations on prism graphs. For $c \geq 0.5$, we observe consensus for all simulations on prism graphs. For $c < 0.5$, the steady state is mostly polarized into 2 distinct opinion groups if $N \geq 100$ and can sometimes have more than 2 opinion groups for $N \in \{10, 50\}$. As with our simulations on cycles in Sec. IV B, we observe that large discrepancies in the initial opinion distribution hinder the agents from agreeing with each other through their interactions on a prism graph.

2. Complete multipartite graphs

In this subsection, we consider complete multipartite graphs $K_{N,r}$, where N is an integer multiple of r . We use the values $r = 2, 5, 10$, and we note that one can construe a complete graph K_N (see Sec. IV A) as a complete multipartite graph $K_{N,r}$ with

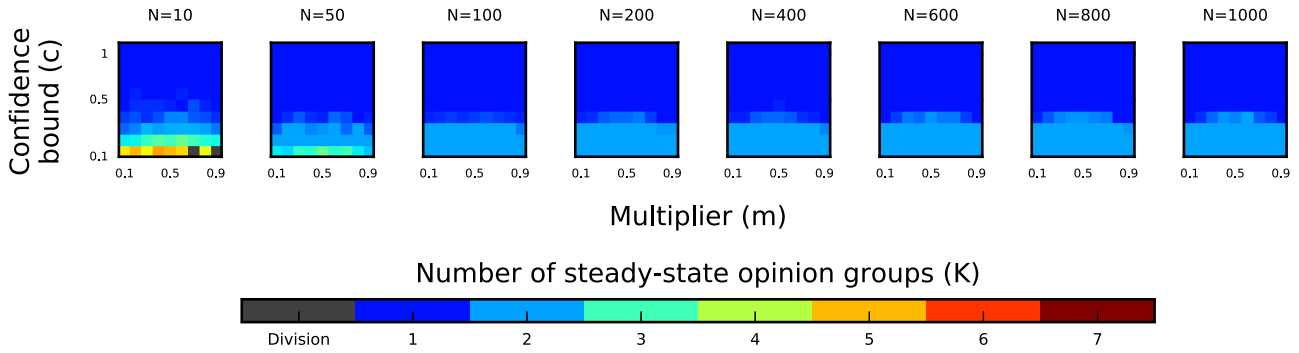


FIG. 18. Number of steady-state opinion groups in simulations on prism graphs for various N .

$r = N$. By varying the value of r , we explore the effect of network density (i.e., the ratio of the number of edges to the maximum possible number of edges [61]) on the behavior of the Deffuant model.

In Fig. 19, we summarize the values of $\ln(T)$ that we observe in our simulations on complete r -partite graphs (with $r = 2, 5, 10$). For a confidence bound $c < 0.6$, most of our simulations do not converge by the bailout time (10^9 iterations), so we conduct regression analysis for $c \geq 0.6$. For $c \geq 0.6$, our regression analysis suggests the model given by Eq. (3), which has the same form as the regression model of complete graphs when $c \geq 0.5$ but has different coefficient values (see Table XIII of Appendix C).

The regression model in Eq. (3) suggests that the behavior of the convergence time on a complete multipartite graph is similar to that on a complete graph. As the number r of partite sets increases, the growth rate of T with respect to N decreases slightly for fixed values of c and m . In other words, as a complete multipartite graph becomes more densely connected, adding agents to it increases the convergence time of the Deffuant model at a slower rate if all other conditions remain the same. Additionally, T increases with $(m - 0.5)^2$ progressively more slowly as r increases.

In Fig. 20, we summarize the number of steady-state opinion groups in our simulations on complete r -partite graphs (with $r = 2, 5, 10$). For $r \in \{5, 10\}$, we observe consensus for all $c \geq 0.5$. We also observe consensus in all of our simulations on bipartite graphs with $c \geq 0.6$, but some simulations fail to converge by the bailout time for $c = 0.5$.

3. Prism graphs with random edges

We consider random graphs generated by the ensemble $Y_{N,s}$ (see Table I) for $s = 0.1$, $s = 0.2$, and $s = 0.3$. We study the effect of adding uniformly random edges on the behavior of the Deffuant model by comparing our simulation results with the ones that we obtained for prism graphs in Sec. B 1.

In Fig. 21, we summarize the values of $\ln(T)$ that we observe in our simulations on $Y_{N,s}$ for $s = 0.1$, $s = 0.2$, and $s = 0.3$. As with our results for prism graphs in Sec. B 1, we observe qualitatively distinct behavior of the convergence time for $c < 0.5$ and $c \geq 0.5$ for the Deffuant model on $Y_{N,s}$. Therefore, we conduct separate regression analyses for these two cases. For $c < 0.5$, our regression analysis suggests the model

$$\ln(T) = \beta_0 + \beta_1 N + \beta_2 N^2 + \beta_3 c + \beta_4 c^2 + \beta_5 (m - 0.5)^2 + \beta_6 N c + \epsilon, \quad (\text{B3})$$

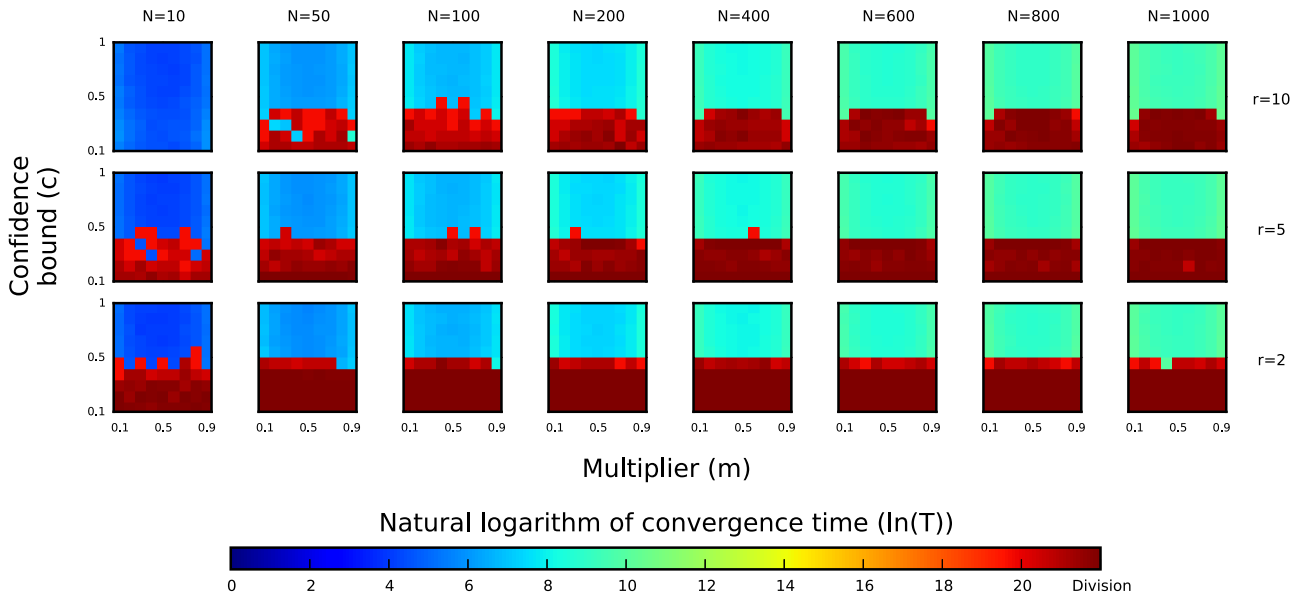


FIG. 19. Convergence times for simulations on N -node complete r -partite graphs (with $r = 2, 5, 10$) for various N .

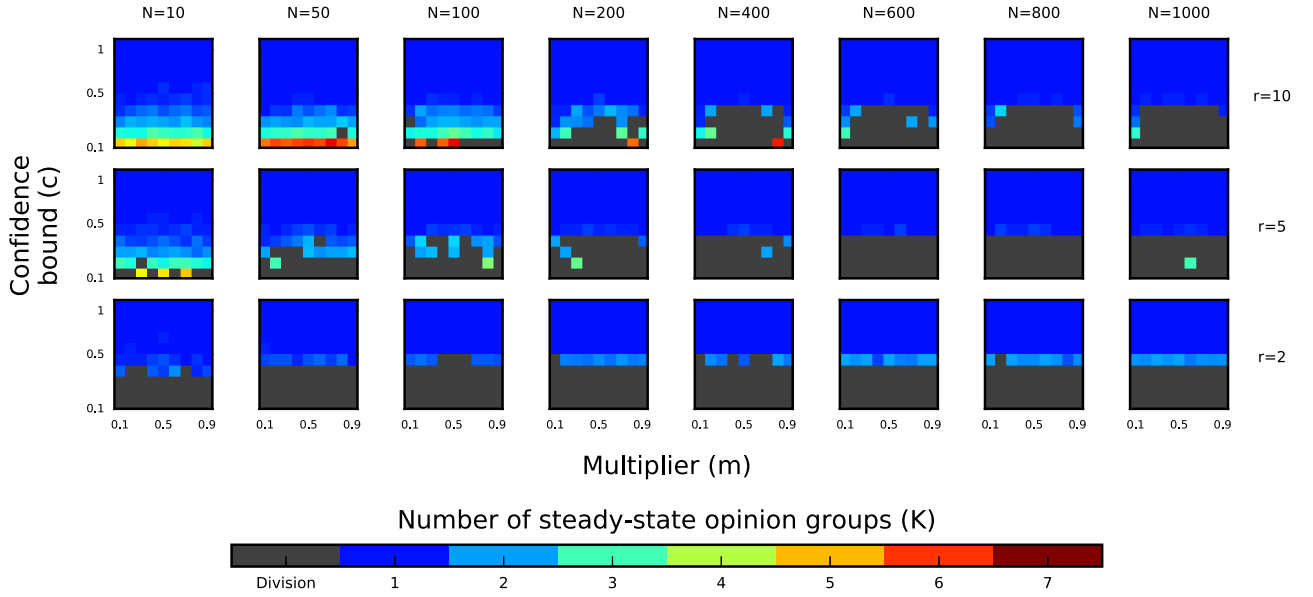


FIG. 20. Number of steady-state opinion groups in simulations on N -node complete r -partite graphs (with $r = 2, 5, 10$) for various N .

where we give our coefficient estimates in Table XIV of Appendix C. For $s = 0.1$, we obtain $AIC \approx -592.1$ and $R^2 \approx 0.9613$; for $s = 0.2$, we obtain $AIC \approx -427.99$ and $R^2 \approx 0.9283$; and for $s = 0.3$, we obtain $AIC \approx -482.58$ and $R^2 \approx 0.9336$. For $c \geq 0.5$, our regression analysis suggests the model

$$\ln(T) = \beta_0 + \beta_1 \ln(N) + \beta_2 c + \beta_3 c^2 + \beta_4 (m - 0.5)^2 + \beta_5 N c + \epsilon, \tag{B4}$$

where we give our coefficient estimates in Table XV of Appendix C. For $s = 0.1$, we obtain $AIC \approx -2596.67$ and $R^2 \approx 0.9914$; for $s = 0.2$, we obtain $AIC \approx -2693.1$ and $R^2 \approx 0.9922$; and for $s = 0.3$, we obtain $AIC \approx -2912.41$ and $R^2 \approx 0.9947$.

The different forms of Eqs. (B3) and (B4) support our conjecture based on data exploration that T undergoes a transition

at $c = 0.5$. The convergence time T tends to increase with N for fixed values of c and m . Moreover, T increases exponentially with $(m - 0.5)^2$ and has a minimum at $m = 0.5$. We also observe that T tends to decrease as c increases for fixed values of N and m . Adding edges uniformly at random to prism graphs decreases T more substantially for $c < 0.5$ than for $c \geq 0.5$.

In Fig. 22, we summarize the number of opinion groups that persist in our simulations on prism graphs with randomly generated extra edges. As we observed for prism graphs, we always obtain consensus on prism graphs with random edges for confidence bound $c \geq 0.5$. However, for $c < 0.5$ and $N \geq 50$, we observe $K \geq 2$, in contrast to $K \approx 2$ for prism graphs. Therefore, when a population's confidence bound is small, adding edges uniformly at random to prism graphs tends to expedite the process of opinions dividing into distinct groups, instead of helping to achieve consensus in a population.

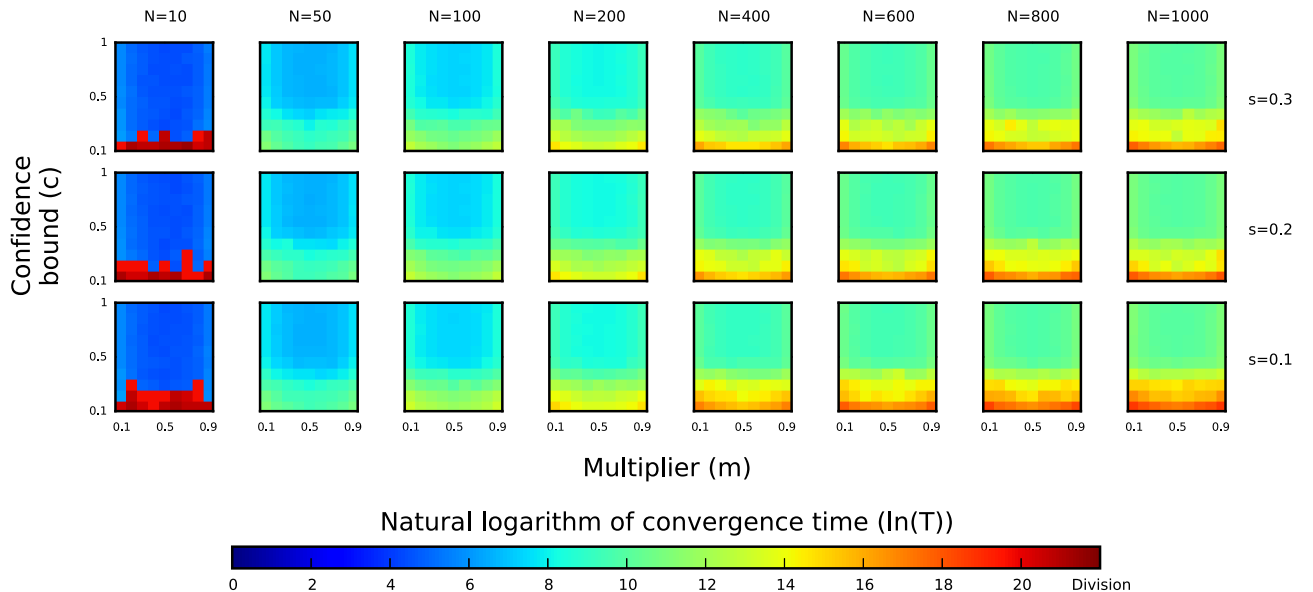


FIG. 21. Convergence times for simulations on $Y_{N,s}$ for $s = 0.1, s = 0.2$, and $s = 0.3$ for various values of N .

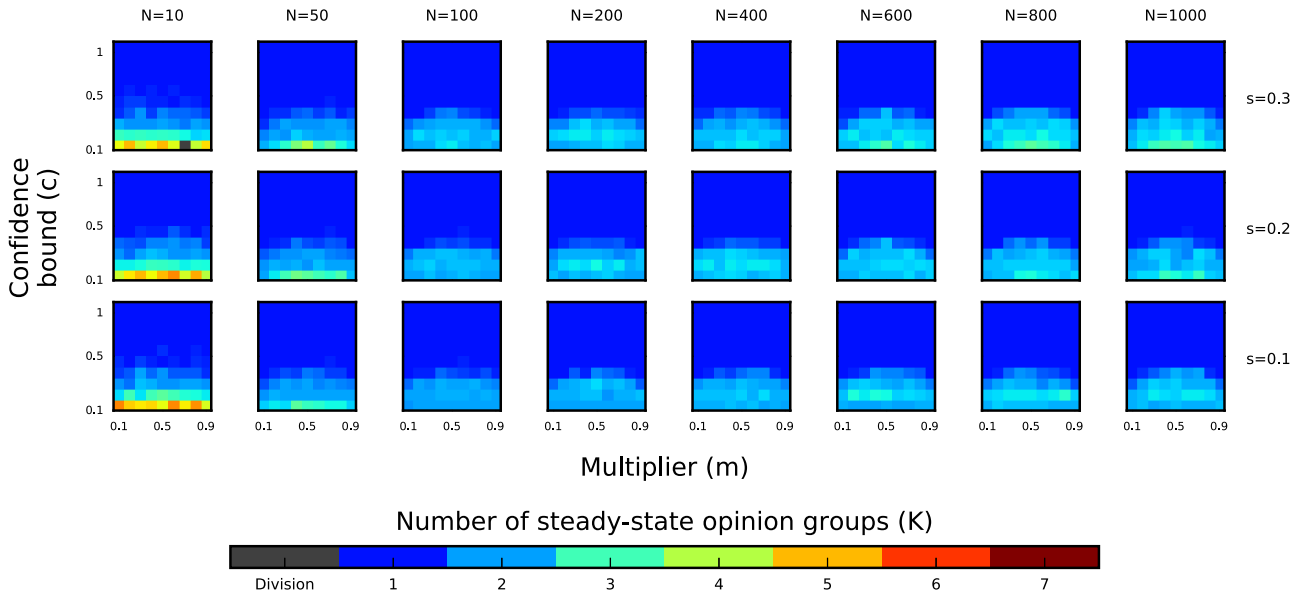


FIG. 22. Number of steady-state opinion groups in simulations on $Y_{N,s}$ for $s = 0.1$, $s = 0.2$, and $s = 0.3$ for various values of N .

4. Facebook friendship networks

We now simulate the Deffuant model on two Facebook “friendship” networks [58]—one of Swarthmore College and the other of the California Institute of Technology (Caltech)—from one day in autumn 2005. We consider the largest connected component (LCC) of each network. For the Swarthmore network, the LCC has 1657 nodes and 61049 edges. The LCC of the Caltech network has 762 nodes and 16651 edges.

In Fig. 23, we summarize the values of $\ln(T)$ that we observe in simulations. For $c < 0.5$, most of the simulations on both networks fail to converge by the bailout time, so we consider only the results of $c \geq 0.5$ in our regression analyses. For the Swarthmore network, we obtain a regression model of

$$T^{-\frac{7}{8}} = \beta_0 + \beta_1 c + \beta_2 c^2 + \beta_3 (m - 0.5)^2 + \epsilon, \quad (B5)$$

where we give our estimates for the coefficients in Table XVI of Appendix C. The values of the AIC and R^2 are -1279.02 and 0.9987 , respectively. For the Caltech network, we obtain a regression model of

$$T^{-\frac{2}{3}} = \beta_1 c + \beta_2 c^2 + \beta_3 (m - 0.5)^2 + \epsilon, \quad (B6)$$

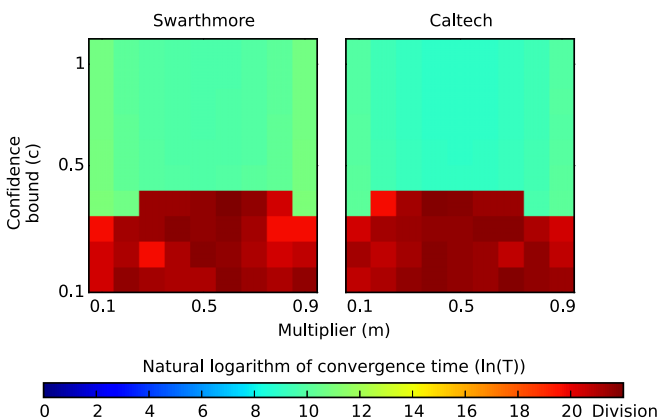


FIG. 23. Convergence times for simulations on the largest connected components of the Swarthmore and Caltech Facebook networks from the FACEBOOK100 data set [58].

where we give our estimates for the coefficients in Table XVII of Appendix C. The values of the AIC and R^2 are -1001.8 and 0.9981 , respectively.

For both networks, the parameters c and m have an intertwined effect on T . Moreover, if m is fixed, the convergence time T tends to decrease as c increases. If c is fixed, T increases with $(m - 0.5)^2$. The convergence time for both of the networks is qualitatively similar to what we observed for cycles with uniformly random edges (see Sec. IVD) of comparable network sizes. This empirical observation suggests that simulating the Deffuant model on random graphs generated by these and similar networks (e.g., WS networks) may yield some useful insights about the convergence time for the Deffuant model on social networks.

In Fig. 24, we summarize the number of steady-state opinion groups in our simulations on the LCCs of the Swarthmore and Caltech Facebook networks. In both networks, consensus occurs for all confidence bounds $c \geq 0.5$. For $c < 0.5$, at least half of the simulations fail to converge within the bailout time, but those that converge suggest that K increases as $c \rightarrow 0$. In

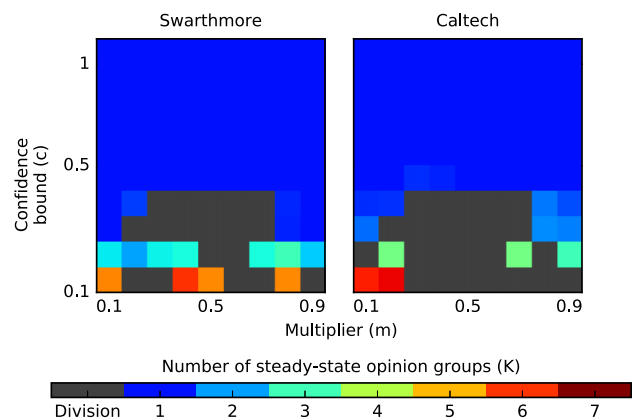


FIG. 24. Number of steady-state opinion groups in simulations on the largest connected components of the Swarthmore and Caltech Facebook networks.

contrast, our simulations of Deffuant dynamics on cycles with uniformly random edges reach a steady state before the bailout time (see Sec. [IV D](#)).

APPENDIX C: BEST-FIT PARAMETERS IN REGRESSION MODELS

In this appendix, we present part of our regression output in Tables [IV–XVII](#). (We use the software environment R [\[87\]](#) for

our regressions.) In Tables [IV–VII](#), [XI](#), [XII](#), [XVI](#), and [XVII](#), we also indicate standard errors, and the column for t values gives the values of the t -statistic for the hypothesis test with the null hypothesis that the corresponding regression coefficient is 0. The column for $\Pr(> |t|)$ in these tables gives the probability that a test statistic is less likely than the observed t value if the null hypothesis is true. A low value of $\Pr(> |t|)$ suggests that it is rare to obtain a result as extreme as the observed value if the coefficient under consideration were 0. In that case, we should keep the corresponding term in the model.

TABLE IV. Estimates of regression coefficients for Eq. (2). In this and subsequent tables, we present estimates for regression coefficients that are accurate to four significant figures. We also give standard errors, t values, and the probabilities that a test statistic is less likely than the observed t value if the null hypothesis is true.

	Estimate	Std. Error	t value	$\Pr(> t)$
β_0	2.139	1.380×10^{-2}	1.550×10^2	$<2 \times 10^{-16}$
β_1	7.124×10^{-4}	5.255×10^{-5}	1.356×10	$<2 \times 10^{-16}$
β_2	-3.763×10^{-7}	4.178×10^{-8}	-9.006	$<2 \times 10^{-16}$
β_3	-9.922×10^{-1}	1.076×10^{-1}	-9.220	$<2 \times 10^{-16}$
β_4	3.696×10^{-4}	8.983×10^{-5}	4.114	4.850×10^{-5}

TABLE V. Estimates of regression coefficients for Eq. (3).

	Estimate	Std. Error	t value	$\Pr(> t)$
β_0	1.865	1.916×10^{-2}	9.734×10	$<2 \times 10^{-16}$
β_1	1.062	3.067×10^{-3}	3.463×10^2	$<2 \times 10^{-16}$
β_2	4.530×10^{-1}	2.398×10^{-2}	1.889×10	$<2 \times 10^{-16}$
β_3	6.262	3.646×10^{-2}	1.718×10^2	$<2 \times 10^{-16}$

TABLE VI. Estimates of regression coefficients for Eq. (4).

	Estimate	Std. Error	t value	$\Pr(> t)$
β_0	-6.313×10^{-1}	3.054×10^{-2}	-2.067×10	$<2 \times 10^{-16}$
β_1	3.018	5.142×10^{-3}	5.870×10^2	$<2 \times 10^{-16}$
β_2	-2.630	6.357×10^{-2}	-4.137×10	$<2 \times 10^{-16}$
β_3	-1.624	7.708×10^{-2}	-2.107×10	$<2 \times 10^{-16}$
β_4	9.371	4.669×10^{-2}	2.007×10^2	$<2 \times 10^{-16}$
β_5	-7.642×10^{-5}	1.713×10^{-5}	-4.461	9.770×10^{-6}

TABLE VII. Estimates of regression coefficients for Eq. (5).

	Estimate	Std. Error	t value	$\Pr(> t)$
β_0	1.505	1.194×10^{-2}	1.261×10^2	$<2 \times 10^{-16}$
β_1	7.361×10^{-2}	2.550×10^{-3}	2.887×10	$<2 \times 10^{-16}$
β_2	-4.931×10^{-5}	1.358×10^{-5}	-3.630	3.110×10^{-4}
β_3	1.336×10^{-8}	7.154×10^{-9}	1.868	6.227×10^{-2}
β_4	-5.129×10^{-2}	1.288×10^{-2}	-3.982	7.790×10^{-5}
β_5	3.154×10^{-2}	8.543×10^{-3}	3.692	2.460×10^{-4}
β_6	-2.430×10^{-1}	4.093×10^{-3}	-5.938×10	$<2 \times 10^{-16}$
β_7	1.396×10^{-1}	3.654×10^{-3}	3.821×10	$<2 \times 10^{-16}$
β_8	1.544×10^{-5}	2.862×10^{-6}	5.395	1.030×10^{-7}

TABLE VIII. Estimates of regression coefficients for Eq. (6). For $s = 0.1$, the Nc term is statistically insignificant, so we drop it.

s	β_0	β_1	β_2	β_3	β_4	β_5	β_6	β_7
0.1	5.485×10^{-1}	-3.140×10^{-2}	6.760×10^{-5}	-2.908×10^{-8}	1.820×10^{-1}	-1.101×10^{-1}	-9.576×10^{-2}	N/A
0.2	2.763×10^{-1}	-2.351×10^{-2}	4.343×10^{-5}	-1.653×10^{-8}	1.779×10^{-1}	-1.084×10^{-1}	-8.901×10^{-2}	-1.008×10^{-5}
0.3	2.031×10^{-1}	-1.977×10^{-2}	3.548×10^{-5}	-1.090×10^{-8}	1.452×10^{-1}	-8.829×10^{-2}	-7.934×10^{-2}	-1.093×10^{-5}

TABLE IX. Estimates of regression coefficients for Eq. (7).

p	β_0	β_1	β_2	β_3	β_4	β_5
0.7	2.098	8.744×10^{-4}	-4.854×10^{-7}	-8.606×10^{-1}	2.294×10^{-1}	N/A
0.8	2.111	8.328×10^{-4}	-4.349×10^{-7}	-7.874×10^{-1}	1.255×10^{-1}	N/A
0.9	2.117	7.901×10^{-4}	-4.327×10^{-7}	-8.926×10^{-1}	1.200×10^{-1}	2.323×10^{-4}

TABLE X. Estimates of regression coefficients, AIC values, and coefficients of determination (R^2) for Eq. (3) from our simulation results on ER random graphs. For comparison, we also include the coefficients for the complete graphs (which arise from the ER model with connection probability $p = 1$) that we studied in Sec. IV A.

p	β_0	β_1	β_2	β_3	AIC	R^2
0.1	1.953	1.050	4.412×10^{-1}	6.362	-3156.1	0.9958
0.2	1.931	1.053	4.500×10^{-1}	6.290	-3194.2	0.9961
0.3	1.918	1.055	4.512×10^{-1}	6.275	-3215.1	0.9962
0.4	1.886	1.060	4.453×10^{-1}	6.270	-3233.7	0.9963
0.5	1.827	1.068	4.548×10^{-1}	6.284	-3209.2	0.9963
0.6	1.870	1.062	4.499×10^{-1}	6.255	-3233.6	0.9964
0.7	1.851	1.065	4.470×10^{-1}	6.242	-3213.7	0.9963
0.8	1.873	1.061	4.555×10^{-1}	6.289	-3267.4	0.9966
0.9	1.838	1.067	4.676×10^{-1}	6.261	-3251.8	0.9965
1	1.865	1.062	4.530×10^{-1}	6.262	-3240.9	0.9964

TABLE XI. Estimates of regression coefficients for Eq. (B1).

	Estimate	Std. Error	t value	$\Pr(> t)$
β_0	1.062×10^2	2.803	3.789×10	$<2 \times 10^{-16}$
β_1	4.319×10^{-1}	6.206×10^{-3}	6.960×10	$<2 \times 10^{-16}$
β_2	-1.790×10^{-4}	4.822×10^{-6}	-3.712×10	$<2 \times 10^{-16}$
β_3	7.759×10	1.830×10	4.239	2.890×10^{-5}
β_4	-5.946×10^2	3.400×10	-1.749×10	$<2 \times 10^{-16}$
β_5	2.839×10^2	5.924	4.792×10	$<2 \times 10^{-16}$
β_6	-1.332×10^{-1}	1.083×10^{-2}	-1.230×10	$<2 \times 10^{-16}$

TABLE XII. Estimates of regression coefficients for Eq. (B2).

	Estimate	Std. Error	t value	$\Pr(> t)$
β_0	2.263	2.634×10^{-2}	8.592×10	$<2 \times 10^{-16}$
β_1	2.072×10^{-1}	3.160×10^{-3}	6.556×10	$<2 \times 10^{-16}$
β_2	-1.212	4.976×10^{-2}	-2.436×10	$<2 \times 10^{-16}$
β_3	7.507×10^{-1}	3.273×10^{-2}	2.294×10	$<2 \times 10^{-16}$
β_4	1.064	1.395×10^{-2}	7.624×10	$<2 \times 10^{-16}$
β_5	-6.056×10^{-5}	9.865×10^{-6}	-6.138	1.650×10^{-9}

TABLE XIII. Estimates of regression coefficients, AIC values, and coefficients of determination (R^2) for Eq. (3) using our simulation results on complete r -partite graphs with $r = 2, 5, 10$.

r	β_0	β_1	β_2	β_3	AIC	R^2
2	1.489	1.093	4.843×10^{-1}	6.553	-2675.68	0.9966
5	1.672	1.074	3.252×10^{-1}	6.415	-2726.16	0.9969
10	1.763	1.068	3.330×10^{-1}	6.305	-2709.59	0.9965

TABLE XIV. Estimates of regression coefficients for Eq. (B3).

s	β_0	β_1	β_2	β_3	β_4	β_5	β_6
0.1	1.225×10	1.240×10^{-2}	-6.048×10^{-6}	-6.132	-1.087×10	6.183	-5.739×10^{-3}
0.2	1.309×10	1.067×10^{-2}	-5.535×10^{-6}	-1.699×10	1.088×10	6.964	-4.199×10^{-3}
0.3	1.353×10	8.670×10^{-3}	-4.073×10^{-6}	-2.060×10	1.764×10	6.879	-3.324×10^{-3}

TABLE XV. Estimates of regression coefficients for Eq. (B4).

s	β_0	β_1	β_2	β_3	β_4	β_5
0.1	3.528	1.200	-4.263	2.628	6.720	-2.061×10^{-4}
0.2	3.300	1.161	-3.242	2.002	6.634	-1.808×10^{-4}
0.3	3.193	1.116	-2.436	1.465	6.671	-5.580×10^{-5}

TABLE XVI. Estimates of regression coefficients for Eq. (B5).

	Estimate	Std. Error	t value	$\Pr(> t)$
β_0	1.338×10^{-4}	5.718×10^{-6}	2.340×10	$< 2 \times 10^{-16}$
β_1	1.419×10^{-4}	1.533×10^{-5}	9.258	6.81×10^{-12}
β_2	-7.964×10^{-5}	9.963×10^{-6}	-7.993	4.13×10^{-10}
β_3	-7.208×10^{-4}	3.989×10^{-6}	-1.807×10^2	$< 2 \times 10^{-16}$

TABLE XVII. Estimates of regression coefficients for Eq. (B6).

	Estimate	Std. Error	t value	$\Pr(> t)$
β_1	6.662×10^{-3}	9.431×10^{-5}	7.063×10	$< 2 \times 10^{-16}$
β_2	-4.201×10^{-3}	1.056×10^{-4}	-3.979×10	$< 2 \times 10^{-16}$
β_3	-7.608×10^{-3}	2.117×10^{-4}	-3.593×10	$< 2 \times 10^{-16}$

- [1] M. O. Jackson, *Social and Economic Networks* (Princeton University Press, Princeton, 2008).
- [2] I. D. Couzin, J. Krause, N. R. Franks, and S. A. Levin, *Nature (London)* **433**, 513 (2005).
- [3] M. H. DeGroot, *J. Am. Stat. Assoc.* **69**, 118 (1974).
- [4] P. Oliver, G. Marwell, and R. Teixeira, *Am. J. Sociology* **91**, 522 (1985).
- [5] D. A. Siegel, *Am. J. Polit. Sci.* **53**, 122 (2009).
- [6] M. O. Jackson and L. Yariv, in *Handbook of Social Economics*, edited by J. Benhabib, A. Bisin, and M. O. Jackson (North Holland Publishing Company, Amsterdam, 2011), pp. 646–678.
- [7] P. Jia, A. MirTabatabaei, N. E. Friedkin, and F. Bullo, *SIAM Rev.* **57**, 367 (2015).
- [8] C. Castellano, S. Fortunato, and V. Loreto, *Rev. Mod. Phys.* **81**, 591 (2009).
- [9] N. E. Friedkin, A. V. Proskurnikov, R. Tempo, and S. Parsegov, *Science* **354**, 321 (2016).
- [10] A. Jadbabaie, Flocking in networked systems, in *Encyclopedia of Systems and Control*, edited by J. Baillieul and T. Samad (Springer-Verlag, London, 2015).
- [11] A. Jadbabaie, J. Lin, and A. S. Morse, *IEEE Trans. Autom. Control* **48**, 988 (2003).

- [12] T. Vicsek and A. Zafeiris, *Phys. Rep.* **517**, 71 (2012).
- [13] M. A. Porter and J. P. Gleeson, *Dynamical Systems on Networks: A Tutorial*, Frontiers in Applied Dynamical Systems: Reviews and Tutorials, Vol. 4 (Springer International Publishing, Cham, 2016).
- [14] D. Acemoglu and A. Ozdaglar, *Dyn. Games Appl.* **1**, 3 (2011).
- [15] P. Sobkowicz, *J. Artif. Soc. Soc. Simul.* **12**(1), 11 (2009).
- [16] B. Kozma and A. Barrat, *Phys. Rev. E* **77**, 016102 (2008).
- [17] P. Clifford and A. Sudbury, *Biometrika* **60**, 581 (1973).
- [18] R. A. Holley and T. M. Liggett, *Ann. Probab.* **3**, 643 (1975).
- [19] P. Holme and M. E. J. Newman, *Phys. Rev. E* **74**, 056108 (2006).
- [20] R. Durrett, J. P. Gleeson, A. L. Lloyd, P. J. Mucha, F. Shi, D. Sivakoff, J. E. S. Socolar, and C. Varghese, *Proc. Natl. Acad. Sci. USA* **109**, 3682 (2012).
- [21] S. Galam, *Eur. Phys. J. B* **25**, 403 (2002).
- [22] B. Latané, *Am. Psychol.* **36**, 343 (1981).
- [23] A. Nowak, J. Szamrej, and B. Latané, *Psychol. Rev.* **97**, 362 (1990).
- [24] K. Sznajd-Weron and J. Sznajd, *Int. J. Mod. Phys. C* **11**, 1157 (2000).
- [25] K. Sznajd-Weron, *Acta Phys. Pol. B* **36**, 2537 (2005).
- [26] G. Deffuant, D. Neau, F. Amblard, and G. Weisbuch, *Adv. Complex Syst.* **3**, 87 (2000).
- [27] R. Hegselmann and U. Krause, *J. Artif. Soc. Soc. Simul.* **5**(3), 2 (2002).
- [28] U. Krause, in *Communications in Difference Equations, Proceedings of the Fourth International Conference on Difference Equations*, edited by S. Elaydi, G. Ladas, J. Popenda, and J. Rakowski (CRC Press, Poznan, 2000), pp. 227–236.
- [29] G. Weisbuch, A. Kirman, and D. Herreiner, *Econ. J.* **110**, 411 (2000).
- [30] G. Weisbuch, G. Deffuant, F. Amblard, and J.-P. Nadal, *Complexity* **7**, 55 (2002).
- [31] T. Millon, M. J. Lerner, and I. B. Weiner, *Handbook of Psychology, Personality and Social Psychology* (John Wiley & Sons, New York, 2003).
- [32] G. Weisbuch, G. Deffuant, and F. Amblard, *Physica A* **353**, 555 (2005).
- [33] J. Lorenz and D. Urbig, *Adv. Complex Syst.* **10**, 251 (2007).
- [34] L. E. Sullivan, in *The SAGE Glossary of the Social and Behavioral Sciences* (SAGE Publishing, New York, 2009).
- [35] D. Fudenberg and J. Tirole, *Game Theory* (MIT Press, Cambridge, USA, 1995).
- [36] M. O. Jackson and Y. Zenou, in *Handbook of Game Theory*, Vol. 4 (North-Holland Publishing Company, Amsterdam, 2014).
- [37] J. Lorenz, in *Communications of the Laufen Colloquium on Science 2007*, edited by A. Ruffing, A. Suhrer, and J. Suhrer (Shaker Publishing, Maastricht, 2007), [arXiv:0806.1587](https://arxiv.org/abs/0806.1587).
- [38] M. F. Laguna, G. Abramson, and D. H. Zanette, *Complexity* **9**, 31 (2004).
- [39] J. Lorenz, *Physica A* **355**, 217 (2005).
- [40] G. Weisbuch, *Eur. Phys. J. B* **38**, 339 (2004).
- [41] S. Fortunato, *Int. J. Mod. Phys. C* **15**, 1301 (2004).
- [42] M. E. J. Newman, *Networks: An Introduction* (Oxford University Press, Oxford, 2010).
- [43] Y. Gandica, M. del Castillo-Mussot, G. J. Vázquez, and S. Rojas, *Physica A* **389**, 5864 (2010).
- [44] M. Jalili, *Physica A* **392**, 959 (2013).
- [45] D. Stauffer and H. Meyer-Ortmanns, *Int. J. Mod. Phys. C* **15**, 241 (2004).
- [46] E. Ben-Naim, P. L. Krapivsky, and S. Redner, *Physica D* **183**, 190 (2003).
- [47] J. Lorenz, *Int. J. Mod. Phys. C* **18**, 1819 (2007).
- [48] G. Deffuant, F. Amblard, G. Weisbuch, and T. Faure, *J. Art. Soc. Soc. Simul.* **5**(4), 1 (2002).
- [49] G. Deffuant, F. Amblard, and G. Weisbuch, [arXiv:cond-mat/0410199](https://arxiv.org/abs/cond-mat/0410199).
- [50] T. Kurahashi-Nakamura, M. Mäs, and J. Lorenz, *J. Artif. Soc. Soc. Simul.* **19**, 7 (2016).
- [51] J.-P. Bouchaud, C. Borghesi, and P. Jensen, *J. Stat. Mech.* (2014) P03010.
- [52] J. Lorenz, *Complexity* **15**, 43 (2010).
- [53] S. Fortunato, V. Latora, A. Pluchino, and A. Rapisarda, *Int. J. Mod. Phys. C* **16**, 1535 (2005).
- [54] C. G. Antonopoulos and Y. Shang, [arXiv:1710.09371](https://arxiv.org/abs/1710.09371).
- [55] A. Parravano, A. Andina-Díaz, and M. A. Meléndez-Jiménez, *PLoS ONE* **11**, e0164323 (2016).
- [56] A. Nordio, A. Tarable, C. F. Chiasserini, and E. Leonardi, *IEEE Trans. Netw. Sci. Eng.* (2017), doi:10.1109/TNSE.2017.2760016; [arXiv:1710.00530](https://arxiv.org/abs/1710.00530).
- [57] E. N. Gilbert, *Ann. Math. Stat.* **30**, 1141 (1959).
- [58] A. L. Traud, P. J. Mucha, and M. A. Porter, *Physica A* **391**, 4165 (2012).
- [59] A. L. Traud, E. D. Kelsic, P. J. Mucha, and M. A. Porter, *SIAM Rev.* **53**, 526 (2011).
- [60] J. S. Juul and M. A. Porter, [arXiv:1707.07187](https://arxiv.org/abs/1707.07187).
- [61] D. B. West, *Introduction to Graph Theory* (Prentice Hall, Upper Saddle River, NJ, 2001), 2nd ed.
- [62] D. Jacobmeier, *Int. J. Mod. Phys. C* **17**, 1801 (2006).
- [63] J. R. Cameron, *Am. J. Orthopsychiatry* **48**, 140 (1978).
- [64] S. Chess and A. Thomas, *Origins and Evolution of Behavior Disorders: From Infancy to Early Adult Life* (Harvard University Press, Cambridge, USA, 1987).
- [65] B. Chestnut, *The 9 Types of Leadership: Mastering the Art of People in the 21st Century Workplace* (Post Hill Press, New York, 2017).
- [66] S. Fortunato and D. Hric, *Phys. Rep.* **659**, 1 (2016).
- [67] M. A. Porter, J.-P. Onnela, and P. J. Mucha, *Notices of the AMS* **56**, 1082 (2009).
- [68] B. Kozma and A. Barrat, *J. Phys. A: Math. Theor.* **41**, 224020 (2008).
- [69] F. T. Boesch and Z. R. Bogdanowicz, *Int. J. Comput. Math.* **21**, 229 (1987).
- [70] G. Chartrand and P. Zhang, *Chromatic Graph Theory* (CRC Press, Boca Raton, 2008).
- [71] D. J. Watts and S. H. Strogatz, *Nature (London)* **393**, 440 (1998).
- [72] M. A. Porter, *Scholarpedia* **7**, 1739 (2012).
- [73] J. D. Hunter, *Comput. Sci. Eng.* **9**, 90 (2007).
- [74] M. E. J. Newman and D. J. Watts, *Phys. Rev. E* **60**, 7332 (1999).
- [75] B. Bollobás and F. R. K. Chung, *SIAM J. Discrete Math.* **1**, 328 (1988).
- [76] A. Alai, M. A. Purvis, and B. T. R. Savarimuthu, in *Proceedings of the 2008 IEEE/WIC/ACM International Conference on Web Intelligence and Intelligent Agent Technology* (IEEE Computer Society, Sydney, 2008), pp. 394–397.
- [77] F. Amblard and G. Deffuant, *Physica A* **343**, 725 (2004).
- [78] S. Lehmann and Y.-Y. Ahn, editors, *Spreading Dynamics in Social Systems* (Springer-Verlag, to be published), available at <https://socialcontagionbook.github.io>.

- [79] C. Crawford, L. Brooks, and S. Sen, in *Proceedings of the 12th International Conference on Autonomous Agents and Multiagent Systems*, edited by T. Ito, C. Jonker, M. Gini, and O. Shehory (ACM, New York, 2013), pp. 1225–1226.
- [80] G. Chen, H. Cheng, C. Huang, W. Han, Q. Dai, H. Li, and J. Yang, *Phys. Rev. E* **95**, 042118 (2017).
- [81] M. Kivelä, A. Arenas, M. Barthelemy, J. P. Gleeson, Y. Moreno, and M. A. Porter, *J. Complex Networks* **2**, 203 (2014).
- [82] P. Holme and J. Saramäki, *Phys. Rep.* **519**, 97 (2012).
- [83] H. Sayama, I. Pestov, J. Schmidt, B. J. Bush, C. Wong, J. Yamanoi, and T. Gross, *Comput. Math. Appl.* **65**, 1645 (2013).
- [84] C. M. Bishop, *Pattern Recognition and Machine Learning* (Springer-Verlag, New York, 2006).
- [85] D. A. Freeman, *Statistical Models: Theory and Practice* (Cambridge University Press, Cambridge, UK, 2005).
- [86] H. Akaike, *IEEE Trans. Autom. Control* **19**, 716 (1973).
- [87] R Project for Statistical Computing, <http://www.R-project.org>.
- [88] G. E. P. Box and D. R. Cox, *J. R. Stat. Soc. Ser. B* **26**, 211 (1964).
- [89] J. W. Osborne, *Practical Assessment, Research and Evaluation* **15**(12), 1 (2010).
- [90] R. D. Cook, *Technometrics* **19**, 15 (1977).
- [91] H. S. M. Coxeter, *Bull. Am. Math. Soc.* **56**, 413 (1950).